Experimental investigation of tensile and bond strength for a GFRP–SSWM hybrid wraps

V. J. Kalyani, D. D. Joshi, P. V. Patel
Department of Civil Engineering, Institute of Technology, Nirma University, Ahmedabad 382481, India
20ftphde48@nirmauni.ac.in, https://orcid.org/0009-0001-2760-0239
digesh.joshi@nirmauni.ac.in, http://orcid.org/0000-0002-3230-8208
paresh.patel@nirmauni.ac.in, http://orcid.org/0000-0002-2946-2212

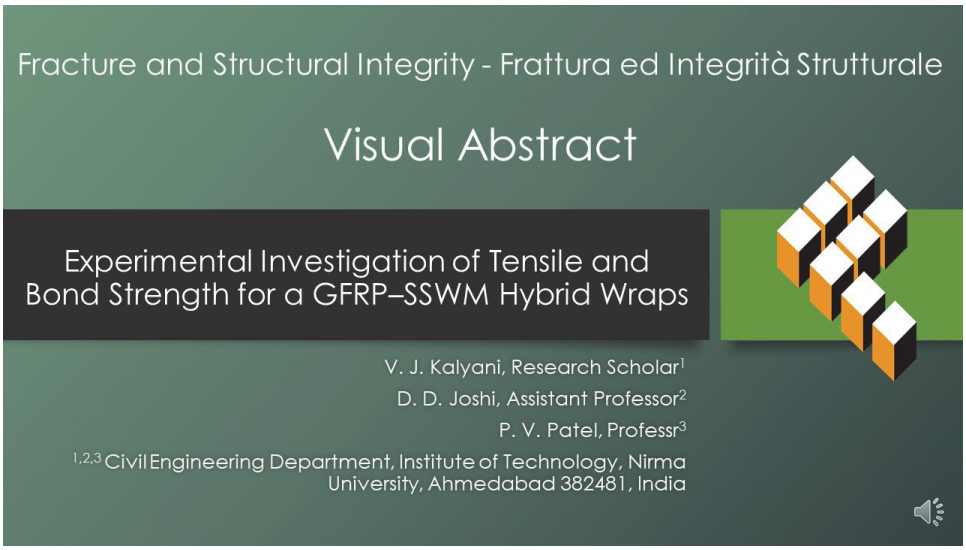

Citation: Kalyani, V. J., Joshi, D. D., Patel., P. V., Experimental investigation of tensile and bond strength for a GFRP–SSWM hybrid wraps, Fracture and Structural Integrity, 74 (2025) 89-114.

Received: 21.05.2025
Accepted: 03.07.2025
Online first: 10.08.2025
Published: 10.2025

KEYWORDS. Glass Fiber Reinforced Polymer (GFRP), Stainless Steel Wire Mesh (SSWM), Hybrid wraps, Tensile Test, Bond Test, Mechanical Properties, Epoxy adhesives.

INTRODUCTION

Fiber-reinforced polymer (FRP) materials are widely used in civil engineering for strengthening and retrofitting existing concrete structures. With ageing infrastructure and increasing exposure to environmental degradation, there is a growing need to enhance the durability, strength, and serviceability of structural systems. Strengthening becomes especially important in cases involving construction defects, changes in codal requirements, modifications in usage, or damage due to fire or accidental loads. Among various strengthening techniques, externally bonded reinforcement (EBR) using FRPs has gained prominence due to its ease of installation, high strength-to-weight ratio, minimal alteration to the existing geometry, corrosion resistance, and improved structural performance in terms of strength. A wide range of FRP

composites have been developed and applied over the past two-three decades. Commonly used types include Aramid FRP (AFRP), Basalt FRP (BFRP), Carbon FRP (CFRP), and Glass FRP (GFRP). Among them, GFRP is particularly attractive due to its high strain capacity and cost-effectiveness. E-glass fibers, in particular, are widely used because they are 10 to 30 times less expensive than CFRP, making them a suitable choice for large-scale applications [1-2]. Several studies have confirmed the substantial improvement in load-carrying capacity and ductility of structural members when strengthened with FRPs. In recent years, the use of CFRP, GFRP, and their hybrid forms available as sheets, strips, rods, grids, and tendons has gained momentum. These materials are bonded to structural elements such as beams, slabs, and columns using various adhesives to improve performance. Despite their advantages, a major limitation of FRP systems is the premature debonding from the concrete surface, which prevents full utilization of their strength. The performance of FRP at elevated temperatures during the event of fires is vulnerable and area of concern that should be addressed by researchers.

To address limitations associated with conventional fiber-reinforced polymer (FRP) systems and to enhance composite action, hybrid retrofitting strategies combining different FRP types or integrating FRPs with other materials have emerged as a promising alternative [3]. Numerous studies have investigated the mechanical performance of such hybrid composites under varied conditions. Hawileh et al. [4] examined the influence of elevated temperatures on the tensile strength, modulus of elasticity, and failure behavior of carbon, glass, and hybrid carbon-glass FRP laminates. Their results demonstrated that hybrid systems exhibited superior thermal stability and mechanical property retention compared to single-fiber laminates, making them suitable for fire-resistant strengthening applications. Wu et al. [5] assessed the tensile fatigue behavior of conventional and hybrid FRP sheets under cyclic loading and reported that hybrid combinations, especially carbon-glass FRP, improved fatigue resistance and delayed failure progression. Additionally, other experimental studies have explored different hybrid configurations, such as the inclusion of S-glass fibers in jute-based composites [6], hybridization of glass fiber reinforced epoxy with stainless steel fibers [7], and multi-phase composites using aluminium reinforced with stainless steel wire mesh and glass fiber [8], glass and jute fiber reinforced composites [9] etc. These investigations reported improved mechanical performance, highlighting the effectiveness of hybrid composites in structural applications. Further, Saidane et al. [10] investigated the hybridization effect of flax and glass fibers on diffusion kinetics and tensile mechanical behavior of epoxy-based composites, highlighting improved tensile performance and moisture resistance in hybrid configurations.

The bond between the laminate and concrete surface plays a critical role in the overall effectiveness of structural strengthening systems. ACI 440.2R-17 [11] offers detailed guidance on evaluating bond strength between FRP systems and concrete, including design recommendations and interface load transfer criteria. Obaidat et al. [12] investigated key parameters influencing bond behavior between externally bonded FRP and concrete, providing valuable insights into interface mechanics and anchorage effectiveness. McIsaac et al. [13] examined the influence of resin type and bio content on the bond strength of FRP wet layup systems, highlighting the significant role of adhesive characteristics in determining bond performance. Nakaba et al. [14] conducted double-face shear bond tests on 36 concrete specimens strengthened on both sides using carbon and aramid fiber fabrics. The study results showed that bond strength increased with the stiffness of the FRP, while variations in the putty layer thickness had minimal effect on the overall load capacity. Yuan et al. [15] investigated the bond performance of hybrid FRP sheets composed of carbon and basalt fibers, externally bonded to concrete, focusing on bond strength and associated failure modes. Their findings showed that hybridization could optimize both strength and ductility at the FRP concrete interface. Huang et al. [16] investigated the bond characteristics of hybrid flax-glass fiber reinforced epoxy composites bonded to laminated veneer lumber, emphasizing that the selection and combination of fiber types significantly influence joint strength and bond performance.

Apart from tensile test and bond behaviour, different configurations of hybrid composites were also explored for strengthening of structural elements such as beams. Choobbora et al. [17] evaluated the flexural performance of RC beams strengthened with hybrid CFRP-BFRP sheets, demonstrating significant improvements in load-carrying capacity and ductility up to 75% and 108%, respectively compared to control and CFRP only strengthened beams. Bai et al. [18] experimentally and analytically investigated the flexural behaviour of RC beams strengthened with hybrid carbon - PET FRP and U-strip anchorages, reporting significant improvements in strength and ductility, along with a validated theoretical model for load-deflection prediction. Lin et al. [19] investigated the flexural performance of RC beams strengthened with five different configurations of hybrid FRP sheets composed of aramid, glass, and carbon fibers. The study reported up to a 30.2% increase in load-carrying capacity, while also highlighting a reduction in ductility with increased layering. Additionally, tensile tests were conducted to evaluate the mechanical properties of each hybrid configuration. Xiong et al. [20] investigated RC beams strengthened with hybrid carbon - glass FRP sheets and found that the hybrid system significantly enhances ductility with minimal reduction in stiffness compared to CFRP only strengthening.

Alternatively, stainless-steel wire mesh (SSWM) has been explored as a strengthening material due to its promising bond performance with concrete and superior behaviour at elevated temperatures. Kumar and Patel [21] were among the first to propose SSWM as a cost-effective alternative to FRPs for strengthening circular plain concrete columns. More recently,

Raiyani et al. [22] demonstrated that partial wrapping with SSWM significantly improves the compressive strength and crack control of concrete cylinders, and they proposed an analytical model to predict the compressive strength of SSWM confined concrete. Ferro et al. [23] studied aluminium matrix composites reinforced with SSWM and observed that while metallurgical bonding enhances ductility, interfacial defects and intermetallic formations can reduce mechanical performance, emphasizing the need for surface treatment and optimized mesh geometry. Harba et al. [24] conducted a numerical study on circular RC columns strengthened with CFRP wraps under concentric and eccentric loading, confirming that increased confinement levels enhance load-carrying capacity and reduce strength loss due to eccentricity.

From the available literature, it is observed that several studies have explored effectiveness of different hybrid composite configurations prepared using variety of material. However, very limited research has been reported on hybrid wraps combining GFRP with SSWM. Hybrid composites incorporating GFRP material and SSWM can offer a promising solution for structural strengthening by addressing the limitations of individual materials. These composites combine the high strength and corrosion resistance of GFRP with the ductility, cost-effectiveness and superior temperature resistance of SSWM, providing an effective alternative for retrofitting applications. Therefore, the present study mainly focuses on investigating the mechanical performance of hybrid GFRP-SSWM wraps through tensile testing in accordance with ASTM D3039 [25], and bond behaviour using test assembly indigenously developed at Civil Engineering Department, Nirma University. Furthermore, fractographic analysis of tested coupon specimens is also carried out to gain deeper insight into failure mechanisms. Based on the findings of this study, the developed hybrid wraps can be effectively utilized for the structural strengthening applications such as flexural and shear enhancement of reinforced concrete beams and confinement of columns. They can also be used for strengthening structural elements exposed to corrosive environment or elevated temperature.

EXPERIMENTAL PROGRAM

The primary objective of this study is to investigate the mechanical behavior of GFRP, SSWM, and hybrid GFRP-SSWM wraps. A total of 42 coupon specimens are prepared for tensile testing in accordance with ASTM D3039, and 48 dumbbell shaped specimens are prepared for bond strength evaluation. The GFRP-SSWM hybrid wraps are developed in the laboratory through a hand layup technique following several trials to ensure proper bonding between layers. Mechanical characterization includes tensile testing to assess ultimate tensile strength, rupture strain, and failure patterns. The study also investigates the influence of two key parameters: (i) the number of reinforcement layers (two and three layers) and (ii) the type of epoxy adhesive Sikadur 330 and Sikadur 30 LP. These parameters are considered to study their combined effect on the tensile and bond performance of both the individual and hybrid wrap configurations.

Materials

For the preparation of test specimens, a 900 GSM unidirectional GFRP fabric is utilized. The technical specifications of the GFRP, as provided by the manufacturer, are summarized in Tab. 1. SSWM is locally available in rolled or cut sheet forms. The technical properties of SSWM, as supplied by the manufacturer, are also presented in Tab. 1. A typical microscopic view of GFRP and SSWM materials considered for the study is presented in Fig. 1(a) and Fig. 1(b), respectively. Based on prevailing market rates, GFRP sheets typically cost around Indian Rupee (INR)1250 per m², whereas stainless steel wire mesh (SSWM) is more economical, priced at approximately INR 650 per m². This represents a cost reduction of nearly 48-50% for SSWM compared to GFRP. Additionally, SSWM is often locally sourced, which reduces transportation and procurement costs. By partially replacing GFRP layers with SSWM in hybrid wraps, the overall material and retrofitting costs can be reduced without compromising mechanical performance. This cost-efficiency, combined with GFRP's high strength along with SSWM's superior ductility and temperature resistance, makes the hybrid system a technically and economically viable solution for structural strengthening.

(a) (b)

Figure 1: Material considered for the study: (a) GFRP (Glass Fiber Reinforced Polymer), and (b) SSWM (Stainless Steel Wire Mesh).

Sikadur 30 LP and Sikadur 330 are two-component thixotropic epoxy resin adhesive composed of a resin and a hardener. SIKADUR 30 LP demonstrates excellent bonding performance with a wide range of substrates, including steel, cast iron, FRP plates, masonry, aluminium, stone, concrete, and timber. Similarly, Sikadur 330 offers strong adhesion characteristics suitable for bonding FRP laminates to various structural surfaces. The technical specifications of epoxy adhesives Sikadur 30 LP and Sikadur 330 are presented in Tab. 1.

Material	Designation	Density (GSM)	Fabric design thickness (mm)	Tensile Strength (MPa)	Elastic modulus (GPa)	Elongation in break (%)
GFRP 900 GSM	G	900 g/m²	0.58	2700	73	5.00
SSWM 40 × 32	S	1175 +/- 25 g/m²	0.25 per wire	693.80	151.23	4.50
Sikadur 30 LP	Sikadur 30 LP	1.8 ± 0.1 kg/liter (Part A+B mixed)	-	≥ 25 after 7 days of curing	~ 10	-
Sikadur 330	Sikadur 330	1.3 ± 0.1 kg/liter (Part A+B mixed)	-	≥ 30 after 7 days of curing	~ 3.5	0.90

Table 1: Technical properties of materials

M-25 grade of concrete is considered for preparation of dumbbell shaped specimens. The concrete mix is designed in accordance with IS 10262:2019 to achieve a target compressive strength of 31.6 MPa at 28 days. The mix proportions by weight for cement, fine aggregates, and coarse aggregates are 400.87 kg/m³, 823.78 kg/m³, and 938.88 kg/m³, respectively. The water to cement ratio (w/c) is maintained at 0.50.

Preparation of specimens

A total of 42 coupon specimens are prepared and tested under normal room temperature to evaluate their mechanical properties. The specimens are divided into two main groups based on the epoxy adhesive used: Sikadur 30 LP and Sikadur 330. Each group is further subdivided according to the number of laminate layers - two layers and three layers. For each specimen configuration, three samples are prepared, resulting in 21 specimens per epoxy group. The different coupon specimen configurations considered for tensile test are summarized in Tab. 2.

Sr. No.	Specimen Configuration	Description of material used	Sikadur 30 LP	Sikadur 330
			No. of Specimens	No. of Specimens
1	GG	Two layers of GFRP	3	3
2	GS	One layer of GFRP and One layer of SSWM	3	3
3	SS	Two layers of SSWM	3	3
4	GGG	Three layers of GFRP	3	3
5	GSG	Two layers of GFRP outside with one layer of SSWM between them	3	3
6	SGS	Two layers of SSWM outside with one layer of GFRP between them	3	3
7	SSS	Three layers of SSWM	3	3
			TOTAL	42

Table 2: Different configurations of coupon specimen for tensile test.

Coupon specimens measuring 500 mm in length and 100 mm in width are prepared using a specially fabricated tension assembly. Initially, GFRP and SSWM sheets are cut to 700 mm length and 100 mm width to fit within the tension assembly frame, enabling the fabrication of specimens with these dimensions. Two plates with screw nut assemblies are fixed on both outer sides to secure the specimens. Long screws and nuts at the ends of these plates are tightened to apply tension, ensuring the GFRP and SSWM layers are firmly pressed together. After tensioning, epoxy adhesive is uniformly applied on the specimen surface using a steel spatula. A schematic diagram showing the dimensions of coupons is presented in Fig. 2(a), while typical photographs of the specimen preparation using the tension assembly frame are shown in Figs. 2(b) to 2(d).
The assembled coupon specimens are allowed to cure under ambient conditions for 24 hours. After curing, the specimens are removed from the assembly frame, and excess GFRP and SSWM are trimmed to obtain final specimens with an effective bonded length of 500 mm. Tensile tests are performed using a UTM after a minimum curing period of 7 days. However, hybrid coupon specimens prepared using the tension assembly frame exhibit differing behaviour during testing, as shown

in Fig. 3(a), with GFRP and SSWM layers failing at different locations. Further, fractographic analysis of the coupon specimens prepared using the tension assembly frame is conducted using a digital microscope. A visible gap between the GFRP and SSWM layers is observed at the failure region of GS specimens, as shown in Fig. 3(b), indicating inadequate interfacial bonding. The examination of failure surfaces confirms the absence of effective hybrid action, primarily due to insufficient adhesion between the constituent layers. These findings highlight the limitations of the specimens prepared using tension assembly frame and suggest the need for alternative method to ensure proper bonding and enhanced mechanical performance of hybrid specimens. As a result, preparation of hybrid coupon specimen using tension assembly frame is discontinued.

Figure 2: Schematic representation of coupon specimen & process of specimen preparation using tension assembly frame

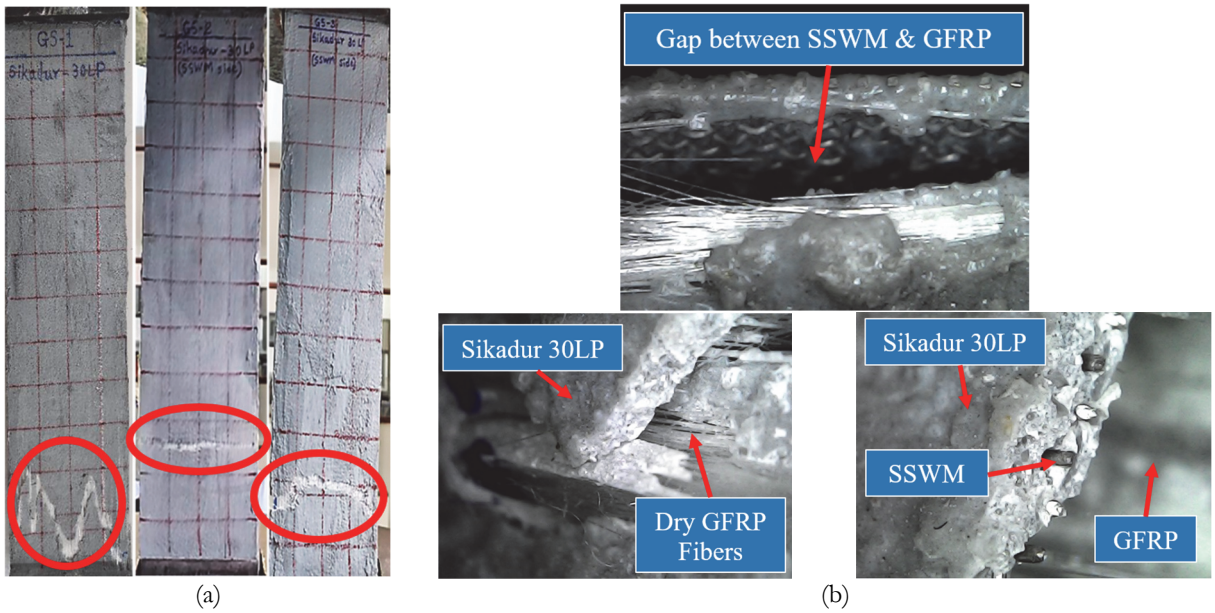

Figure 3: Failure and Fractographic assessment of hybrid coupon specimens prepared using tension assembly frame.

In the subsequent trial, a customized hand lay-up assembly is employed for the preparation of hybrid GS coupon specimens. A mould is fabricated using PVC sheets, as illustrated in Figs. 4(a) to 4(c), and its components are assembled using mechanical fasteners such as screws and nut-bolts. The top cover is then removed to facilitate the placement and inspection of pre-cut fibre materials within the specimen cavity (Fig. 4(c)). Specimen development begins with the uniform application of epoxy adhesive within the 500 mm × 100 mm mould cavity using a steel applicator, as shown in Fig. 4(d). For hybrid specimens, a layer of SSWM is first embedded into the freshly applied adhesive (Fig. 4(e)). A hand roller is used to eliminate air voids and surface irregularities, ensuring proper adhesion. A second layer of epoxy is then uniformly applied over the SSWM layer (Fig. 4(f)), followed by placement of the GFRP fabric layer (Fig. 4(g)). This layer is also compacted using a

roller to ensure strong interfacial bonding. As shown in Fig. 4(h), a final layer of epoxy adhesive is applied over the GFRP to complete the lay-up.

The mould's top cover is repositioned (Fig. 4(i)), and uniform mechanical pressure is applied using nut-bolts and weighted plates (Fig. 4(j)) to enhance consolidation of laminate layers and minimize air entrapment. After curing for 24 hours under ambient conditions, the assembly is disassembled and the hybrid coupon specimen is carefully extracted. The mould is then reassembled for subsequent specimen preparation. To complete the test specimen, steel end tabs measuring 100 mm × 100 mm × 6 mm are bonded to both ends using the same adhesive, as shown in Fig. 4(k), to facilitate gripping during tensile testing. The final hybrid coupon specimens measure 500 mm in length and 100 mm in width, with an effective gauge length of 300 mm, satisfying the requirements of ASTM D3039 [25] for tensile testing. All experimental results of tensile test performed on coupon specimens of different configurations, reported in the present study correspond exclusively to specimens prepared using this second approach.

Figure 4: Illustrative photographs of step-wise procedure for development of hybrid GFRP-SSWM wrap.

A total of 48 bond specimens are cast, prepared, and tested in this experimental investigation to evaluate the bond strength between concrete and various strengthening materials under ambient conditions. The specimens are primarily categorized into two groups based on the type of adhesive used: Sikadur 30 LP and Sikadur 330, consistent with the classification used for the coupon specimens. Within each adhesive group, the specimens are further subdivided according to the strengthening configurations employed for bond testing, as detailed in Tab. 3.

Dumbbell-shaped specimens are cast using M25 grade concrete. A schematic representation of the specimen dimensions is shown in Fig. 5(a). The formwork is prepared from 17 mm thick white PVC sheets, as shown in Fig. 5(b). A uniform 1 mm gap is maintained between the two parts of each dumbbell specimen. A typical photograph of the casting of specimen is provided in Fig. 5(c). Specimens are demoulded after 24 hours, and subjected to water curing for 28 days. Following curing,

the specimens are cleaned to remove surface debris. The top and bottom surfaces of the specimen are smoothened using an electric grinding machine to eliminate surface irregularities and weak concrete as illustrated in Fig. 5(d). Subsequently, they are cleaned using cloth and an air blower. The two parts of the dumbbell specimen are positioned in place, and a layer of epoxy adhesive is applied uniformly to the bonding surface. A 500 mm × 100 mm laminate is placed over the adhesive layer and compacted using a specialized hand roller to ensure proper adhesion and removal of air voids. Another layer of epoxy is applied over the first laminate, followed by the placement and rolling of the second laminate layer. A final layer of adhesive is then applied over the second laminate as shown in Fig. 5(e). After 24 hours of ambient curing, the specimen is turned over, and the same procedure is repeated on the opposite face. Additional fabric layers, as per the requirement for three layers strengthening, are applied in the same sequence on both sides. After strengthening, the specimens are allowed to cure under ambient conditions for 7 days before testing. A typical specimen ready for testing is shown in Fig. 5(f).

Sr. No.	Specimen Configuration	Description of material used	Sikadur 30 LP	Sikadur 330
			No. of Specimens	No. of Specimens
1	GG	Two layers of GFRP	3	3
2	GS	One layer of GFRP and one layer of SSWM with SSWM on top	3	3
3	SG	One layer of SSWM and one layer of GFRP with GFRP on top	3	3
4	SS	Two layers of SSWM	3	3
5	GGG	Three layers of GFRP	3	3
6	GSG	Two layers of GFRP with one layer of SSWM between them	3	3
7	SGS	Two layers of SSWM with one layer of GFRP between them	3	3
8	SSS	Three layers of SSWM	3	3
		TOTAL		**48**

Table 3: Different strengthening configurations for bond test.

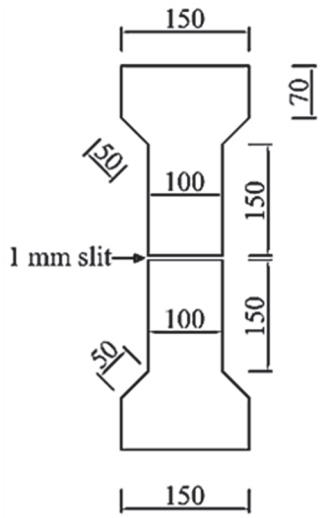

(all dimensions are in mm)

(a)

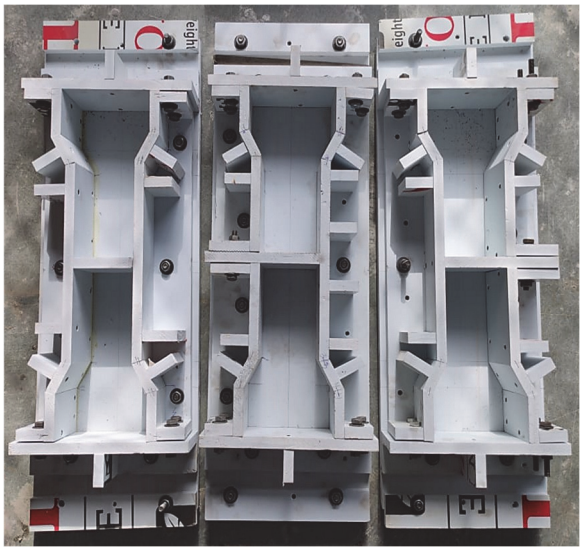

(b)

(c)

(d) (e) (f)

Figure 5: Dimension and procedure for preparation and strengthening of dumbbell shaped specimen for bond test

Experimental test setup

A 400 kN capacity Universal Testing Machine (UTM) is used to perform tensile tests on the coupon specimens. The UTM is regularly calibrated to ensure measurement accuracy. The placement of the coupon specimen between the upper and lower crossheads of the UTM, as part of the tensile test setup, is shown in Fig. 6. All tensile tests are conducted in accordance with ASTM D3039 [25] under ambient temperature conditions, at a constant displacement rate of 1-2 mm/s. The UTM is equipped with a calibrated load cell that records the applied force digitally through a data acquisition system. Load and displacement data are displayed in real time on a digital meter and recorded simultaneously. A video recording stand is used to document the failure behavior of the specimens during testing, and the footage is utilized to assist in the analysis of failure mechanisms.

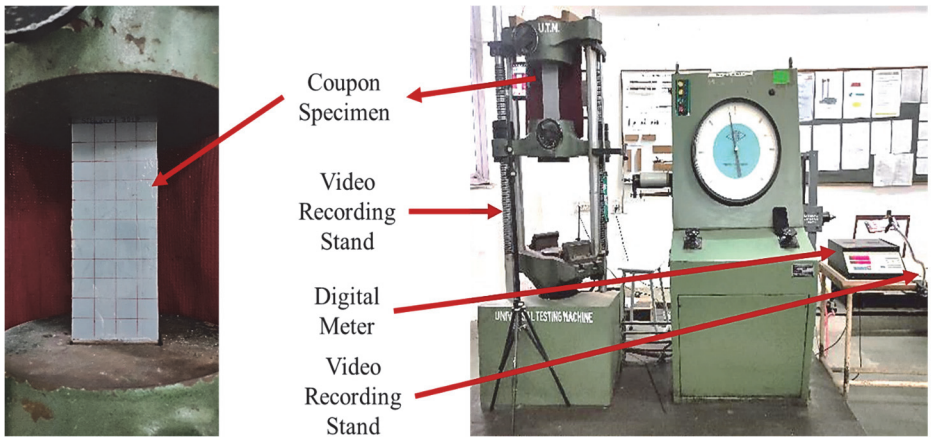

Figure 6: Test setup for tensile test on coupon specimens

After 7 days of ambient curing, the dumbbell specimens are subjected to monotonic loading using a universal testing machine (UTM), as shown in Fig. 7. The compressive load from the UTM is transferred as a direct axial tensile force to the dumbbell specimen through a specially designed and indigenously developed frame assembly. The load is applied at a constant displacement rate of 1-2 mm/min. A 100 kN compression type load cell, mounted at the top of the frame assembly, records the applied load. Displacement is measured using two Linear Variable Differential Transformers (LVDTs) mounted symmetrically on either side of the specimen. Additionally, a 5 mm gauge length electrical resistance strain gauge is installed at the center of the strengthened surface along the longitudinal axis to capture strain readings under tensile loading. Real time data of load, displacement, and strain are recorded using a digital data acquisition system.

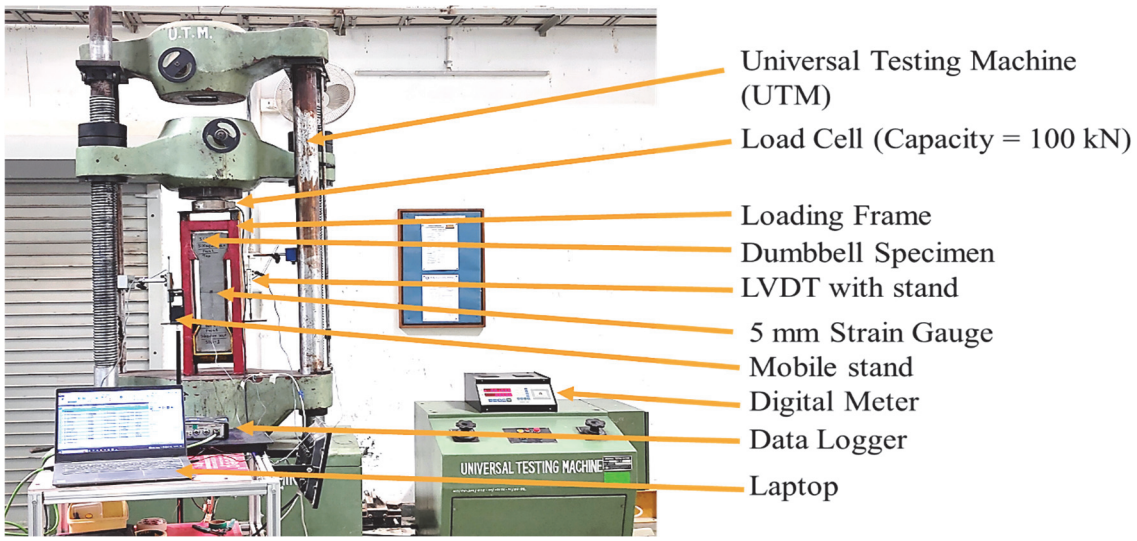

Figure 7: Test setup for bond test on dumbbell shaped specimens.

RESULTS AND DISCUSSION

Tensile test on coupon specimens

Tensile tests is performed on coupon specimens of size 500 mm length × 100 mm width in accordance with ASTM D3039 [25]. The performance of coupon specimens is evaluated in terms of ultimate load, displacement corresponding to ultimate load, ultimate tensile strength, rupture strain stiffness, modulus of elasticity and failure pattern. For each configuration, three specimens are considered and average results of three specimen are presented in Tab. 4.

Bonding Material	Specimen Configuration	Average Ultimate Load kN	Average Displacement at Ultimate Load mm	Average Stiffness kN/mm	Average Ultimate Tensile Strength MPa	Average Rupture Strain μm/m	Average Modulus of Elasticity MPa
Sikadur 30 LP	GG	50.25	5.17	12.59	210.25	0.01723	15810.45
	GS	31.74	8.99	5.54	142.97	0.02997	8641.48
	SS	10.45	13.82	1.06	52.51	0.04607	1742.59
	GGG	62.23	4.03	17.93	213.12	0.01344	18410.42
	GSG	55.67	4.91	11.64	198.82	0.01638	12471.83
	SGS	36.20	6.64	6.49	149.59	0.02213	8050.26
	SSS	15.56	12.92	2.03	57.42	0.04308	2250.55
Sikadur 330	GG	44.99	5.08	11.12	212.22	0.01694	16323.70
	GS	29.20	5.24	5.69	140.38	0.01748	8200.20
	SS	9.90	11.35	1.35	51.03	0.03784	2079.46
	GGG	61.43	3.49	16.42	222.57	0.01031	15449.90
	GSG	48.28	4.83	10.89	187.13	0.01514	13463.43
	SGS	34.27	5.03	6.53	147.72	0.01676	8444.52
	SSS	13.75	10.84	1.39	55.00	0.03613	2249.34

Table 4: Results of the tensile test performed on coupon specimens.

Tab. 5 presents the statistical indicators such as standard deviation and coefficient of variation (CoV) for the key mechanical parameters obtained from the tensile tests. The results exhibit good consistency across most specimen configurations, with CoV values well below 5%, reflecting high repeatability and reliability of the measured outcomes. Slightly higher CoV values up to 8.15 are observed in certain three-layer configurations such as GGG and SSS, particularly when prepared using epoxy adhesive Sikadur 330; however, they also remained within the commonly accepted threshold of 10%, indicating acceptable variability. Furthermore, the narrow width of the 95% confidence interval scatter bands presented in the subsequent graphs further reinforces the consistency of the experimental data.

Epoxy	Specimen Configuration	Ultimate Load		Ultimate Tensile Strength		Stiffness		Rupture Strain		Modulus of Elasticity	
		SD	CoV (%)	SD	CoV (%)	SD	CoV (%)	SD	CoV (%)	SD	CoV (%)
Sikadur 30LP	GG	1.44	2.86	6.01	2.85	0.33	2.60	0.0005	2.62	173.26	1.10
	GS	0.54	1.71	2.45	1.70	0.11	1.93	0.0003	1.11	43.48	0.50
	SS	0.05	0.47	0.25	0.47	0.01	0.25	0.0001	0.25	70.07	4.02
	GGG	1.05	1.69	3.60	1.67	0.57	3.19	0.0004	3.22	478.66	2.60
	GSG	0.75	1.35	2.68	1.33	0.31	2.65	0.0004	2.66	159.24	1.28
	SGS	0.26	0.73	1.09	0.73	0.12	1.84	0.0004	1.83	99.40	1.23
	SSS	0.06	0.35	0.20	0.36	0.01	0.53	0.0002	0.52	60.62	2.69
Sikadur 330	GG	1.02	2.27	4.81	2.27	0.38	3.45	0.0006	3.46	242.75	1.49
	GS	0.29	0.98	2.28	1.62	0.19	3.32	0.0006	3.32	153.76	1.88
	SS	0.26	2.67	1.36	2.59	0.02	1.42	0.0005	1.41	53.56	2.58
	GGG	1.50	2.45	5.45	2.45	1.34	8.14	0.0009	8.15	106.14	0.69
	GSG	1.35	2.81	5.25	2.73	0.51	4.71	0.0007	4.73	169.01	1.26
	SGS	0.86	2.52	3.71	2.54	0.12	1.77	0.0003	1.79	123.19	1.46
	SSS	0.82	5.95	3.27	5.87	0.06	4.65	0.0017	4.65	173.58	7.72

SD = Standard Deviation, CoV = Coefficient of Variance

Table 5: Statistical indicators for mechanical parameters evaluated during tensile test.

The average ultimate load results for all configurations indicates that the number and type of reinforcing layers significantly influence the tensile performance of the coupon specimens. For specimens bonded with Sikadur 30 LP, the highest ultimate load of 62.23 kN is observed for the GGG configuration, followed closely by 55.67 kN for GSG and 50.25 kN for GG specimen. These results suggest that multiple layers of GFRP, substantially enhance load carrying capacity of coupon specimens. Among all, SS and SSS configurations, consisting entirely of SSWM, show the lowest load carrying capacity with 10.45 kN and 15.56 kN, respectively, reflecting the relatively lower tensile strength contribution of SSWM compared to GFRP. However, hybrid configurations such as GS, SGS, and GSG exhibit a balanced performance, bridging the gap between the high strength of GFRP and the ductility of SSWM. For instance, the GSG configuration bonded with Sikadur 30 LP achieves an average ultimate load of 55.67 kN, which is approximately 89.46% of the GGG configuration, while incorporating only two GFRP layers and one SSWM layer instead of three GFRP layers. Similarly, the GS configuration records an average load of 31.74 kN, which is 63.16% of GG, despite replacing one GFRP layer with a single SSWM layer. This highlights the efficiency of the hybrid layup in achieving high tensile strength with reduced GFRP usage.

A similar trend is observed for specimens bonded using Sikadur 330, where the GGG configuration again exhibits the highest average ultimate load of 61.43 kN, followed by 48.28 kN for GSG and 44.29 kN for GG specimen. The hybrid GS configuration registers an ultimate load of 29.20 kN, which is approximately 64.10% of the GG specimen. However, when compared to the SS specimen (9.90 kN), the GS hybrid achieves nearly three times the load capacity, indicating the significant enhancement that a single layer of GFRP provides even in a hybrid assembly. Similarly, the SGS configuration reaches 34.27 kN, which is 149.24% higher as compared to SSS, and closely approaching GG at 76.17% of its strength despite using only one GFRP layer. A comparison of ultimate load capacity observed for different specimen configuration when prepared using Sikadur 30 LP and Sikadur 330, is also presented in Fig. 8(a).

Fig. 8(b) presents the comparison of ultimate tensile strength for coupon specimens of different configurations. Tensile strength is measured as the ratio of ultimate tensile load to the cross-sectional area of the respective wrap configuration. Among all the specimens, the highest tensile strength is observed for GGG specimens for both the epoxy adhesives, followed by specimen GG. For instance, the GGG configuration shows the highest tensile strength of 213.12 MPa for Sikadur 30 LP and 222.57 MPa for Sikadur 330, indicating excellent load-carrying capacity of the GFRP under uniaxial tension. The GG specimens also show comparably high tensile strength for both adhesives, with 210.25 MPa for Sikadur 30 LP and 212.22 MPa for Sikadur 330, further confirming the superior strength contribution of GFRP. In contrast, specimens strengthened only with SSWM layers i.e. SS and SSS, display the lowest tensile strengths. The tensile strength of SS specimen is observed as 52.51 MPa and 51.03 MPa, respectively, when prepared with Sikadur 30 LP and Sikadur 330. This trend remains similar for the three-layer SSS specimens, showing tensile strength of 57.42 MPa and 55.00 MPa respectively, for Sikadur 30 LP and Sikadur 330, reflecting the lower tensile strength of SSWM compared to GFRP. The relatively lower tensile strengths across all coupon specimens, compared to individual material capacities, are influenced by the presence of multiple (3-4) thin layers of epoxy adhesive. The low tensile strength of the adhesive layer, combined with parameters such as specimen dimensions, loading rate, and number of wrap layers etc., contributes to this reduction.

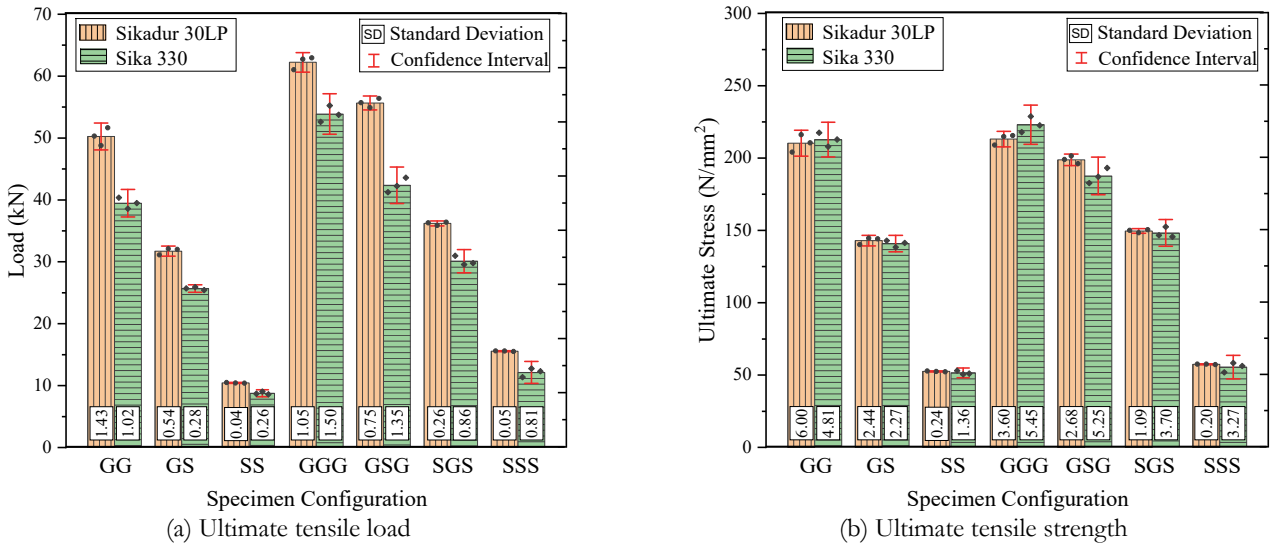

(a) Ultimate tensile load (b) Ultimate tensile strength

Figure 8: Comparison of ultimate load and tensile strength of specimen prepared using adhesive Sikadur 30LP and Sikadur 330

The performance of hybrid configurations (GS, SGS, and GSG) falls between the GFRP-only and SSWM-only specimens. For example, GS exhibits tensile strengths of 142.97 MPa (Sikadur 30 LP) and 140.38 MPa (Sikadur 330), which are significantly higher than SS but notably lower than GG specimens. A similar trend is observed for SGS specimens, where tensile strength reaches to 149.59 MPa and 147.72 MPa, respectively. Interestingly, the GSG configuration shows relatively high tensile strength of 198.82 MPa (Sikadur 30 LP) and 187.13 MPa (Sikadur 330), approaching the performance of pure GFRP specimens, likely due to the dominant presence of GFRP layers on both sides. Slightly higher tensile strengths are observed in GG and GGG specimens bonded with Sikadur 330, indicating its better compatibility with GFRP material. However, Sikadur 30 LP demonstrates greater effectiveness as an adhesive when SSWM layers are present, particularly in hybrid specimens.

The load vs. displacement and stress vs. strain curves for tensile tests on the coupon specimens are shown in Fig. 9(a) and Fig. 9(b), respectively, for Sikadur 30 LP and Sikadur 330 epoxy adhesive. From the graph, it is observed that, among all configurations, the GGG specimens exhibit a relatively steep initial slope, indicating high stiffness, followed by a sudden and brittle failure beyond the ultimate load capacity. In contrast, the SS and SSS specimens display lower stiffness but undergo a more gradual load reduction beyond peak load, reflecting a ductile failure mechanism. When displacement at ultimate load is considered alongside tensile strength, hybrid configurations reveal a more balanced performance between strength and ductility. The GS configuration, while recording lower ultimate load than GG and GGG, exhibits noticeably greater deformation at failure i.e. 8.99 mm and 5.24 mm for Sikadur 30 LP and Sikadur 330, respectively. This represents an increase in displacement of approximately 73.88% and 3.15% compared to the GG specimens, indicating that the integration of SSWM effectively delays brittle failure and enhances energy absorption. The SGS configuration, which features a GFRP layer sandwiched between SSWM layers, also demonstrates enhanced deformability, with ultimate displacements of 6.64 mm and 5.03 mm for Sikadur 30 LP and Sikadur 330, respectively. Similarly, the hybrid GSG specimens show higher displacement at failure than the GGG configuration. Overall, the displacement at peak load for triple layer hybrid configurations increased in a range of 21% to 60% as compared to GGG, depending on the arrangement of layers and type of adhesive used. The higher deflection observed in SGS compared to GSG further highlights the positive contribution of SSWM in improving the ductility of the hybrid wraps.

Stiffness values calculated from the initial linear portion of the load - displacement curves, are presented in Tab. 4 and Fig. 10 for different configurations of coupon specimen. The highest stiffness is obtained for the GGG configuration in both adhesive systems which is 17.93 kN/mm with Sikadur 30 LP and 16.42 kN/mm with Sikadur 330, reflecting the influence of multiple high modulus GFRP layers in minimizing deformation under tensile load. Contrary, specimens prepared entirely from SSWM, such as SS and SSS, exhibit the lowest stiffness values across both adhesive systems. For Sikadur 30 LP, stiffness values for SS and SSS are obtained as 1.06 kN/mm and 2.03 kN/mm, respectively. The same with Sikadur 330 is obtained as 1.35 kN/mm and 1.39 kN/mm, respectively. These results reflect the relatively low modulus and high deformability of SSWM materials. The double layer GG specimen exhibits high stiffness values of 12.59 kN/mm and 11.12 kN/mm for Sikadur 30 LP and Sikadur 330, respectively as compared to hybrid GS specimen. Hybrid configurations exhibit stiffness values intermediate between those of only GFRP and only SSWM specimens, indicating a balanced between rigidity

and ductility. The GSG specimen, for example, shows a stiffness of 11.64 kN/mm with Sikadur 30 LP and 10.89 kN/mm with Sikadur 330, values that are 35.08% and 33.68% lower than the corresponding GGG values, respectively. Similarly, the SGS configuration shows lower stiffness than GSG but higher than GS and SSS, with 6.49 kN/mm and 6.53 kN/mm for Sikadur 30 LP and Sikadur 330, respectively. The GS configuration, which places a single layer of SSWM over GFRP, exhibits lowest stiffness of 5.54 kN/mm and 5.69 kN/mm for Sikadur 30 LP and Sikadur 330, respectively among the hybrid coupon specimen considered for the study. This suggests that the inclusion of SSWM reduces the overall stiffness despite the presence of GFRP layer by improving ductility. Nonetheless, the GS and SGS hybrids provide a balanced performance, offering enhanced ductility without a complete compromise in stiffness. Overall, the stiffness results reinforce the hybrid configurations' mechanical behavior by balancing the strength of GFRP and the ductility of SSWM, making them promising alternative for structural strengthening.

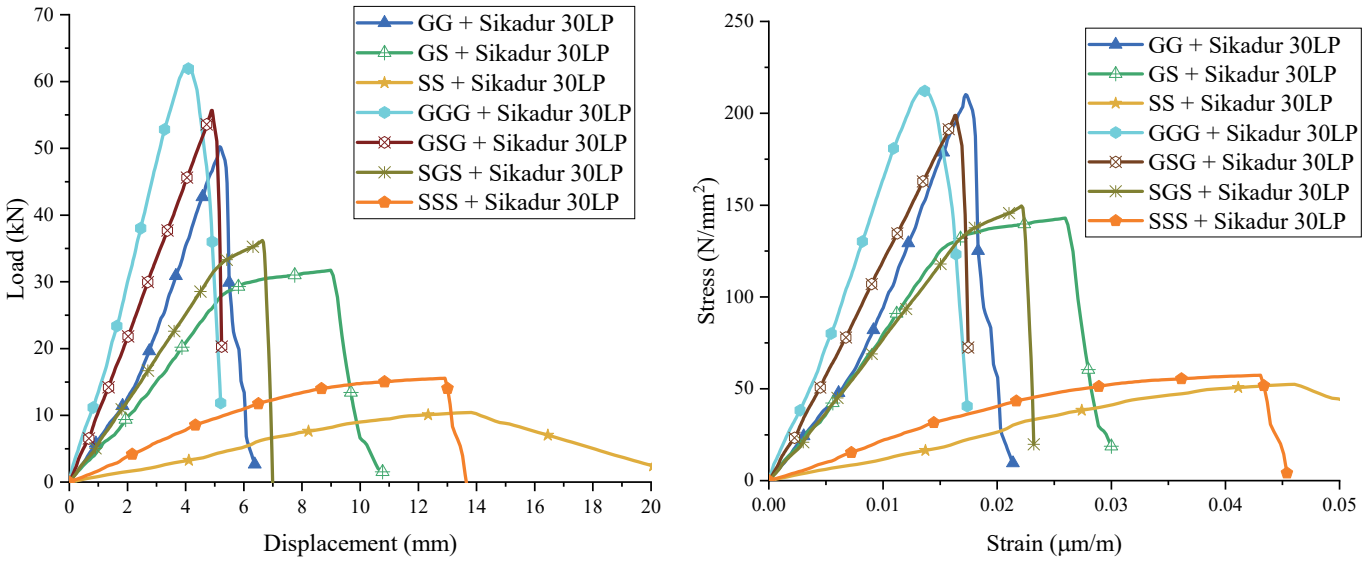

(a) use of Sikadur 30 LP as epoxy adhesive.

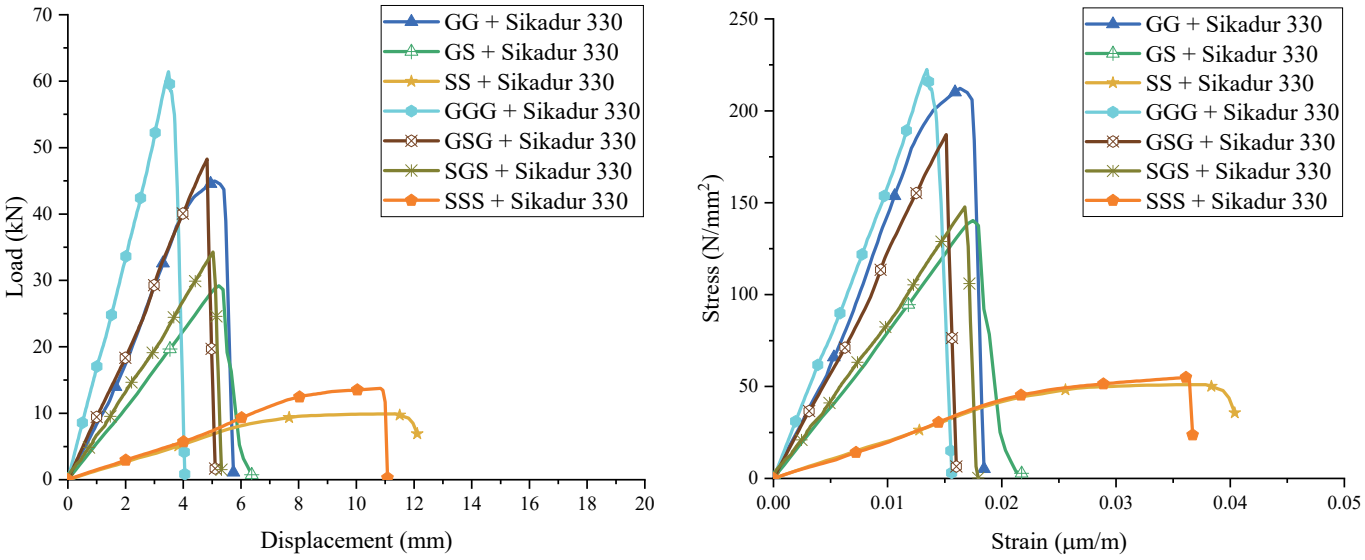

(b) use of Sikadur 330 as epoxy adhesive

Figure 9: Load vs. displacement and stress vs. strain curve for coupon specimen prepared with (a) Sikadur 30LP and (b) Sikadur 330 .

The results of rupture strain are summarized in Tab. 4 as well as presented in Fig. 11(a). Specimens prepared from SSWM (SS and SSS) display the highest rupture strains across both adhesives, reaching values of 0.04607 and 0.04308 µm/m (Sikadur 30 LP) and 0.03784 and 0.03613 µm/m (Sikadur 330), respectively. While, the GGG configuration exhibits the lowest rupture strain at 0.01344 µm/m for Sikadur 30 LP and 0.01031 µm/m for Sikadur 330, reflecting the brittle nature of the GFRP layers. Despite the lower ultimate load carrying capacity, the rupture strain of SSS is approximately 3.21 and

3.50 times higher than that of GGG, respectively, when Sikadur 30 LP and Sikadur 330 epoxy adhesive is used, highlighting the ductile response offered by SSWM. Hybrid configurations demonstrate intermediate rupture strain values, indicating a blending of the ductile and brittle behaviours. Among them, the GS configuration shows a rupture strain of 0.02997 μm/m (Sikadur 30 LP), which is 73.94% higher than GG but 34.95% lesser than SS. Similarly, SGS shows rupture strain of 0.02213 μm/m, which is 64.66% higher than GGG, reflecting the substantial influence of even a single SSWM layer in enhancing deformability. GSG, though composed of two GFRP layers, maintains a rupture strain of 0.01638 μm/m, which is 22% higher than GGG. However, the rupture strain of hybrid specimens SGS and GSG are lesser by 48.63% and 61.98%, respectively, as compared to SSS. Overall, these results highlight that hybrid specimens, particularly GS and SGS, provide a notable improvement in strain capacity, allowing more energy absorption when subjected to uniaxial tensile load and enhancement in ductility and post-yield performance as compared to only GFRP specimens.

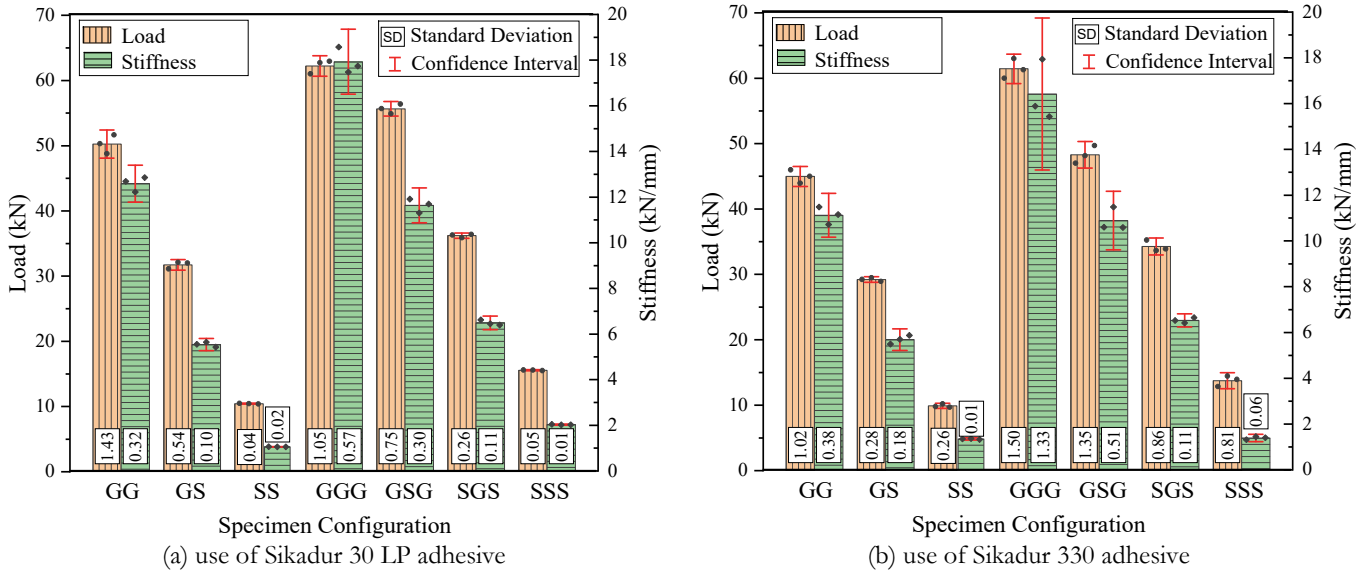

(a) use of Sikadur 30 LP adhesive (b) use of Sikadur 330 adhesive

Figure 10: Comparison of stiffness for coupon specimen prepared with (a) Sikadur 30LP and (b) Sikadur 330

The modulus of elasticity values presented in Tab. 4 and comparison in bar chart form is shown in Fig. 11(b), which reinforces the trends observed in rupture strain. Sepcimens GG and GGG exhibit the highest modulus values, with GGG reaching 18,410.42 MPa (Sikadur 30 LP) and 15,449.90 MPa (Sikadur 330). In contrast, SS and SSS coupon specimens show significantly lower modulus values in a range of 1,742 MPa to 2,250 MPa, indicating a more flexible response under tensile load. The modulus for hybrid configuration fall in mid-range as compared to only GFRP and only SSWM specimen. The modulus of SGS (8,050.26 MPa with Sikadur 30 LP and 8,444.52 MPa with Sikadur 330) lies between that of SSS and GGG, while GSG exhibits elastic modulus values around 12,471.83 MPa and 13,463.43 MPa, respectively, when Sikadur 30LP and Sikadur 330 is used. Compared to GGG, modulus of elasticity is reduced in a range of 12.85% to 56.87% for GSG and SGS specimens. The GS configuration, shows reduction of 45.34% (Sikadur 30LP) and 49.77% (Sikadur 330) in modulus of elasticity as compared to GG configuration. However, the modulus of elasticity for both two-layer and three-layer hybrid specimens is significantly higher as compared to SS and SSS specimens.

The comparative performance between two-layer i.e. GG, GS, SS and three-layer i.e. GGG, GSG, SGS, SSS specimens clearly demonstrates the influence of number of layers on mechanical properties. A three-layer GFRP specimens (GGG) outperforms their two-layer counterparts (GG) in terms of ultimate load capacity and stiffness, due to the additional reinforcing layer of GFRP contributing to higher strength. However, this increase of one additional layer, adversely affect the ductility of the coupon specimen, as reflected by the lower rupture strains and displacement at failure. A two-layer hybrid wrap GS demonstrates superior ductility and energy absorption capacity, while three-layer hybrid configurations such as GSG and SGS generally provide higher ultimate strength and stiffness due to the increased volume of reinforcing materials. For instance, SGS specimen demonstrated 64.66% (sikadur30 LP) and 62.56% (Sikadur 330) higher rupture strain, than GGG while retaining around 58% (sikadur30 LP) and 56% (Sikadur 330) of its ultimate load. It indicates a synergy of strength and ductility for the hybridization of GFRP and SSWM to overcome limitations of individual material. Similar results are also observed for specimen GSG.

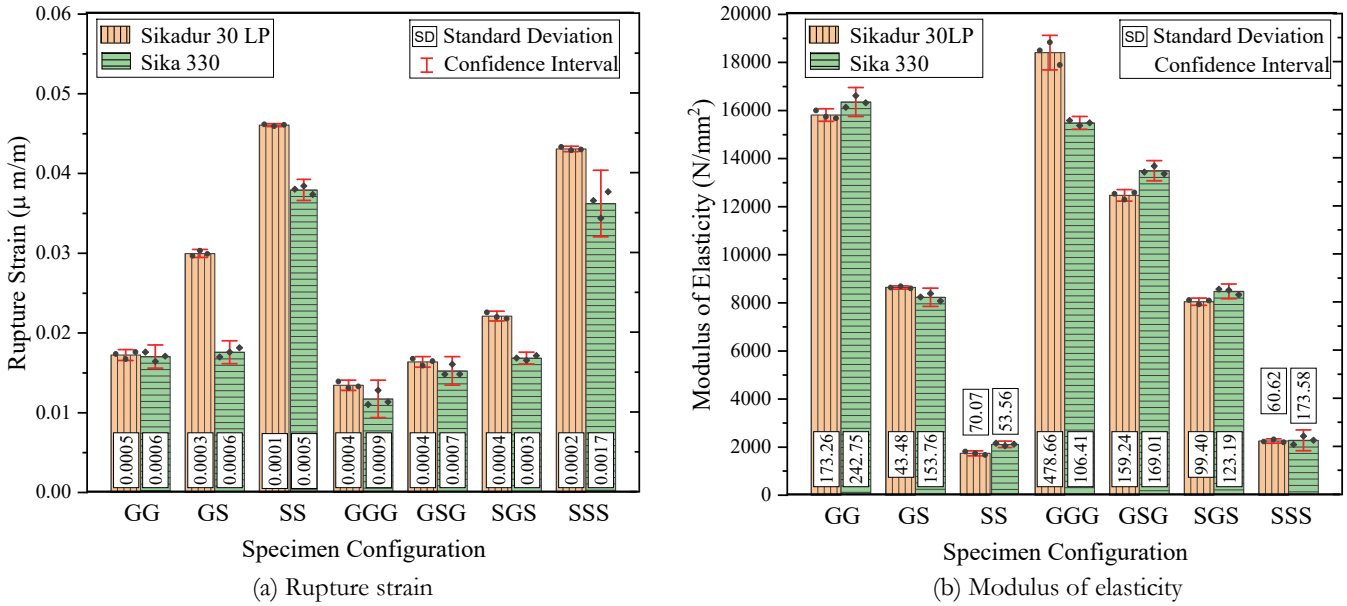

(a) Rupture strain (b) Modulus of elasticity

Figure 11: Comparison of results - mechanical properties of coupon specimen prepared using adhesive Sikadur 30LP and Sikadur 330

Two-layer hybrids specimen GS also show promising results, especially in terms of deformability, achieving up to 73.89% higher displacement than GG when prepared using epoxy adhesive Sikadur 30 LP, with 36.83% reduction in ultimate load capacity. From the results, it is also evident that, rupture strain decreases with increase in number of layers. For any configuration of three-layer wrap, rupture strain is lesser as compared to two-layer wrap. The GS specimens consistently exhibited higher rupture strain and displacement at ultimate load compared to three-layer hybrids, indicating a more gradual failure process. For instance, in the case of Sikadur 30 LP, the GS specimen showed a rupture strain of 0.02997 and displacement of 8.99 mm, both of which were significantly higher than those of GSG (0.01638, 4.91 mm) and SGS (0.02213, 6.64 mm). This trend suggests that increasing the number of stiff GFRP layers often results in a more brittle response. Hence, from a performance-efficiency point of view, the two-layer GS configuration is recommended for a desirable balance, between sufficient strength enhancement with superior ductility compared to its three-layer counterparts.

The type of adhesive also plays an important role on mechanical performance of the coupon specimens. In general, specimens bonded with Sikadur 30 LP exhibited higher ultimate load and displacement at peak load across most configurations compared to those bonded with Sikadur 330. For example, in the GS specimen, Sikadur 30 LP achieved an ultimate load of 31.74 kN, which is approximately 8.70% higher than that obtained with Sikadur 330 (29.20 kN). Similarly, the GS configuration bonded with Sikadur 30 LP recorded a displacement of 8.99 mm, significantly higher than 5.24 mm observed with Sikadur 330, indicating improved ductility and energy absorption capapcity. Moreover, the performance variation between adhesives appears to be dependent on the type of material being bonded. While Sikadur 330 performs effectively in bonding high-modulus GFRP layers, it shows relatively weaker interface compatibility with SSWM, which may be attributed to its lower viscosity and penetration capacity. In contrast, Sikadur 30 LP demonstrates superior bonding characteristics with SSWM, as seen in the higher rupture strains and displacements for SS and SSS configurations. For instance, the SS specimen exhibited a rupture strain of 0.04607 with Sikadur 30 LP compared to 0.03784 with Sikadur 330, indicating a 21.7% increase in strain capacity, which directly reflects the improved adhesive interaction with the steel mesh structure. These trends suggest that Sikadur 30 LP is more suitable for hybrid or SSWM wraps, while Sikadur 330 remains effective for only GFRP dominant configurations.

Failure pattern of coupon specimens

The typical failure patterns observed for coupon specimens prepared using Sikadur 30 LP and Sikadur 330 epoxy adhesives are presented in Fig. 12(a) and Fig. 12(b), respectively. In majority cases, no end tab failures are observed, indicating effective load transfer on specimen through the steel tabs. Failure is mainly observed within the gauge length of the specimen, except few specimens where failure occurred nearer to the tab at top or bottom ends. Specimens such as GG and GGG, comprising multiple GFRP layers, failed abruptly in a brittle manner. This abrupt failure is attributed to fiber breakage within the gauge length and delamination, consistent with their low rupture strain and high modulus of elasticity. In contrast, SSWM and hybrid configurations, presented more progressive failure modes. For GS, SGS and GSG specimens, failure occurred at the

same location and propagated further across the specimen width, which indicates effective bonding across diverse material interfaces and proper hybrid action is achieved. For GS specimen, the gridlines remain largely intact in the lower region, suggesting that the load transfer and stress distribution are quite efficient before complete failure. This type of failure indicates strong interfacial bonding and effective hybrid interaction between the constituent materials.

(a) use of Sikadur 30 LP adhesive

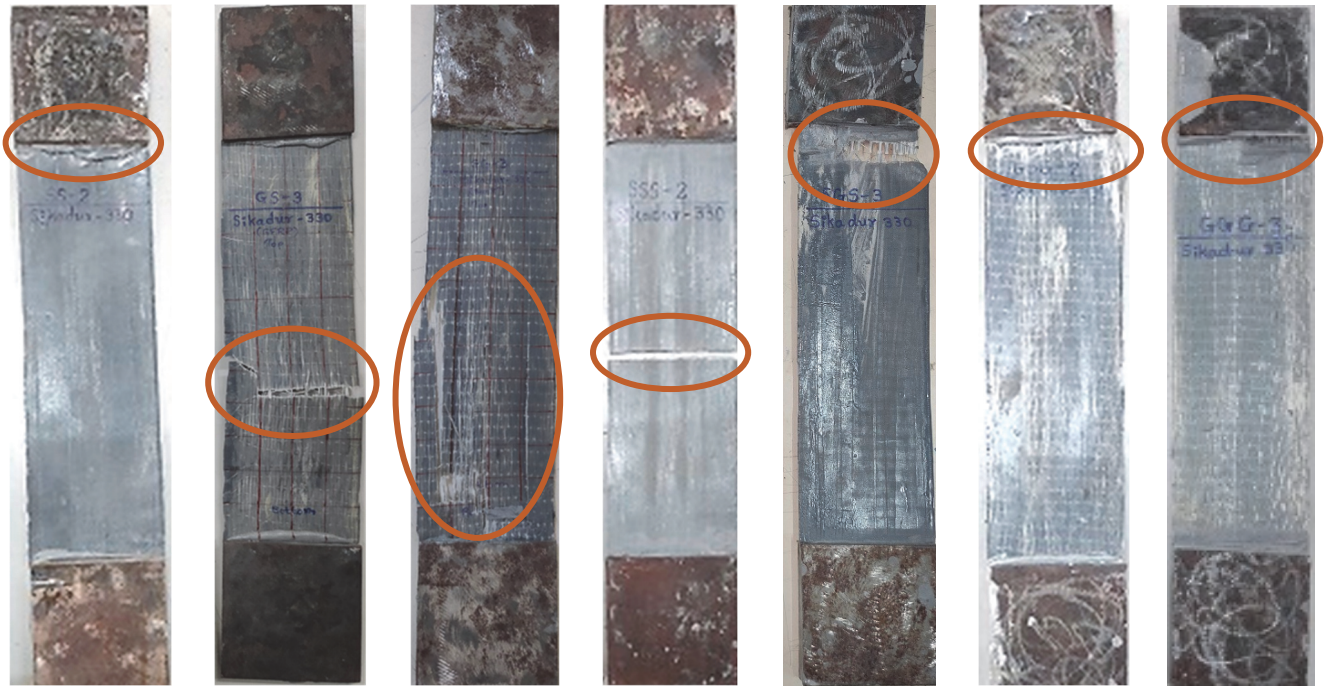

(b) use of Sikadur 330

Figure 12: Failure patterns of coupon specimens prepared using adhesive Sikadur 30 LP and Sikadur 330.

The GFRP layers of GG specimen undergoes fiber pull out and longitudinal splitting rather than complete rupture. The GS specimen prepared with Sikadur 330 displays a more diffuse and irregular failure mode. The fracture line is broader and seems to involve more widespread matrix cracking and potential adhesive failure. The fabric appears frayed, and the fiber pull-out is more significant, which indicates weaker interfacial bonding between the GFRP and SSWM components. The lack of a sharp, cohesive fracture path implies premature failure and ineffective load sharing between layers as compared to epoxy adhesive Sikadur 30 LP. Similar observation from failure pattern of SGS and GSG specimens are noticed. As shown in Fig. 12(a), for SGS specimen, distinct failure localized near the mid-gauge region, with visible cracking, suggesting good adhesive penetration and effective bonding between the layers of GFRP and SSWM materials. In contrast, for Sikadur 330, early peeling and extensive surface delamination is observed in specimen SGS, especially near the tab end, accompanied by visible fiber matrix separation, which indicates inefficient hybrid behaviour.

Fractographic assessment of coupon specimens

Fractographic assessment of the tested coupon specimen is carried out manually using a digital microscope to evaluate the failure mechanisms at the microstructural level. Some of the typical photographs of failure plane, at microscopic level are presented in Fig. 13 for different configurations of two-layer coupon specimens. This assessment is performed on specimens prepared using both Sikadur 30 LP and Sikadur 330 adhesives, for different specimen configurations. The primary objective of this microscopic evaluation is to mechanisms that contributed to the failure of different specimen configurations and bond characteristics between layers at the interface.

In Fig. 13(a), fractographic analysis clearly demonstrates that the SS specimen exhibits a strong interfacial bond with Sikadur 30 LP. It shows distinct impressions and full embedment of the stainless-steel wires within Sikadur 30 LP, along with visible adhesive particles clinging to the mesh, indicating deep penetration and strong interfacial bonding. Fig. 13(b) reveals relatively fewer adhesive remnants and less uniform bonding with Sikadur 330, with wires appearing more exposed. The bonding quality of Sikadur 30 LP with the wire mesh is visibly superior to that of Sikadur 330, suggesting more effective mechanical interlocking and adhesive penetration. Similarly, the difference in Fig. 13(c) and Fig. 13(d), clearly demonstrates significant interfacial debonding and microcracks within the adhesive layer, when GFRP and SSWM are bonded using Sikadur 330. Fig. 13(e) shows fiber breakage and debonding between GFRP and adhesive, indicating brittle failure behavior and poor stress distribution across the GFRP layers bonded with Sikadur 30LP. In contrast, extensive fiber alignment with minimal matrix damage is observed as shown in Fig. 13(f), when GFRP layers are bonded with Sikadur 330, suggesting improved load transfer and more cohesive failure within the GFRP layers.

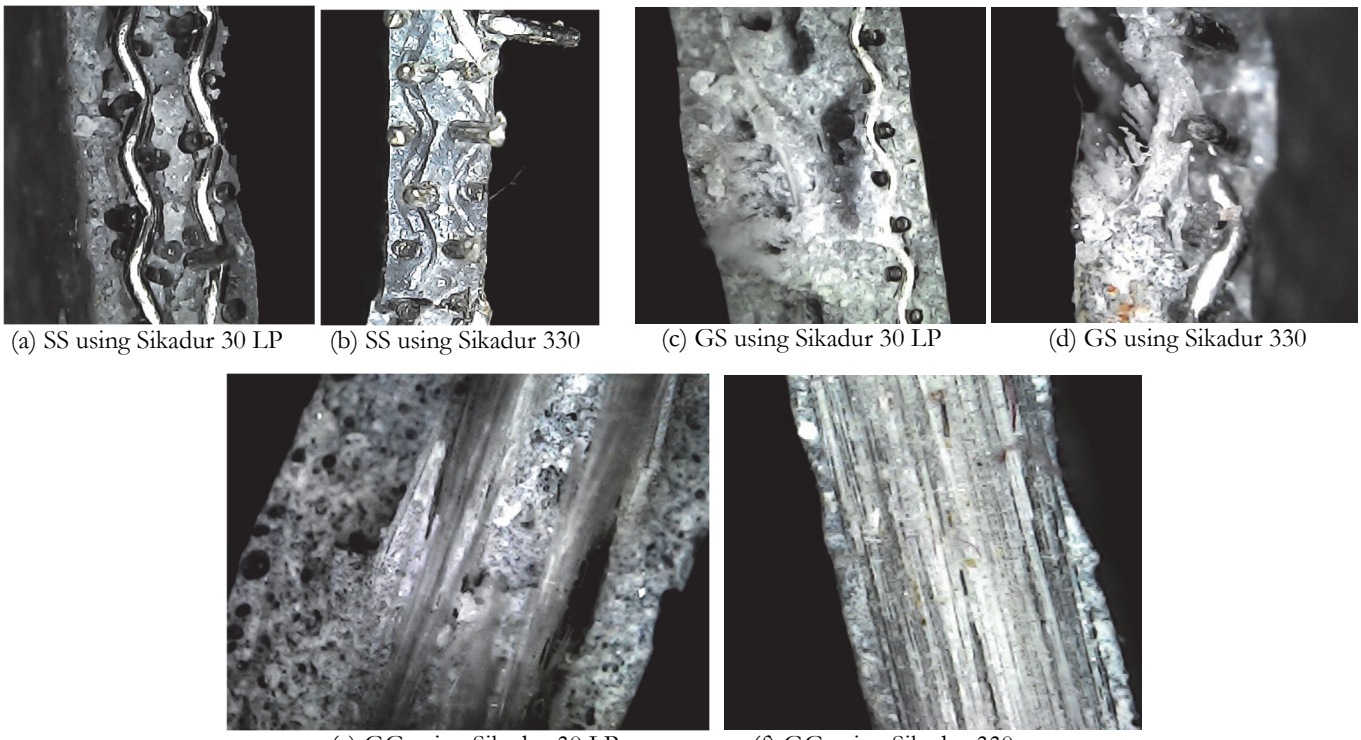

(a) SS using Sikadur 30 LP (b) SS using Sikadur 330 (c) GS using Sikadur 30 LP (d) GS using Sikadur 330

(e) GG using Sikadur 30 LP (f) GG using Sikadur 330

Figure 13: Microscopic views at the failure plane in two-layer coupon specimens.

Fig. 14 presents typical microscopic views at the failure plane in different configurations of three-layer coupon specimens, prepared using Sikadur 30 LP and Sikadur 330. Fig. 14(a) shows that steel wires of the SSWM are clearly embedded and well anchored within the hardened adhesive. Good adhesive penetration around and between the wires is evident, with minimal visible voids. The surface shows no prominent cracks, though minor irregularities and surface texture variations are present. In contrast, Fig. 14(b) shows that steel wires of the SSWM are embedded in the adhesive, but the bonding appears less integrated compared to Sikadur 30 LP. There are visible voids or air pockets around several wires, and in some areas, the adhesive seems to have pulled away or not fully wetted the mesh. The failure of SSWM wires is found to be ductile in nature, as indicated by the characteristic cup and cone morphology.

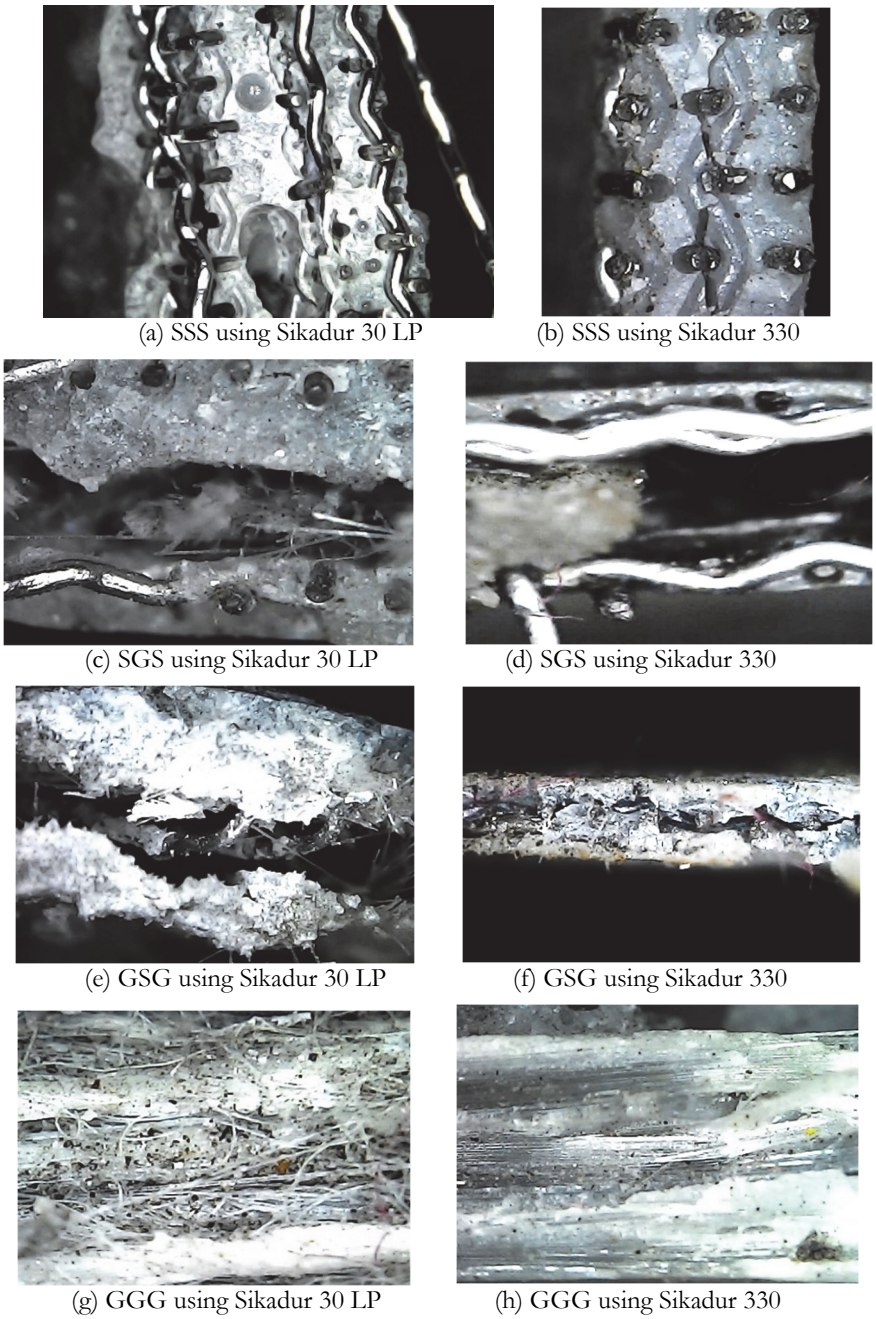

(a) SSS using Sikadur 30 LP (b) SSS using Sikadur 330

(c) SGS using Sikadur 30 LP (d) SGS using Sikadur 330

(e) GSG using Sikadur 30 LP (f) GSG using Sikadur 330

(g) GGG using Sikadur 30 LP (h) GGG using Sikadur 330

Figure 14: Microscopic views at the failure plane in three-layer coupon specimens.

Figs. 14(c) and 14(d) show the failure planes of SGS hybrid specimens bonded with Sikadur 30 LP and Sikadur 330, respectively. In Fig. 14(c), the low viscosity of Sikadur 30 LP appears to facilitate deeper penetration into the SSWM mesh, resulting in a well-formed composite structure. However, this bonding effectiveness does not extend to the GFRP layer, where dry, poorly bonded fibers are evident. Despite this, the residual presence of Sikadur 30 LP near the failure plane

suggests its strong adhesive potential. In contrast, Fig. 14(d) shows that Sikadur 330 forms a stronger and more consistent bond with GFRP layers. However, microscopic assessment reveals poor bonding with the SSWM layer, as indicated by the absence of Sikadur 330 residue on the SSWM wires, highlighting a weakness in adhesive compatibility with metallic reinforcement.

Fig. 14(e) illustrates the failure of a GSG specimen bonded with Sikadur 30 LP. Here, the SSWM layer is observed to have detached from the composite at the failure plane, likely due to insufficient bonding with the adjacent GFRP layers, which appeared dry and ineffective in forming an integrated structure. Conversely, Fig. 14(f), shows the GSG specimen bonded with Sikadur 330, reveals a more cohesive interface. The SSWM layer remains embedded between two well-bonded GFRP layers. Figs. 14(g) and Fig. 14(h) depicts the GGG specimens prepared using Sikadur 30 LP and Sikadur 330, respectively. The GGG specimen bonded with Sikadur 330 demonstrates superior bonding characteristics and cohesive action, attributable to the epoxy's higher viscosity, which facilitates uniform wetting and better fiber consolidation. In contrast, the lower viscosity of Sikadur 30 LP results in less effective fiber engagement and weaker interfacial bonding, as observed microscopically in Fig. 14(g).

Post-failure analysis of all three-layer coupon specimens reveals the occurrence of cracking or debonding within the middle layer, which consisted of either GFRP or SSWM, except in the GGG specimens bonded with Sikadur 330, where such behavior was not observed. It is also observed that wraps prepared using Sikadur 30 LP exhibited a higher prevalence of uneven and dry GFRP fibers compared to those bonded with Sikadur 330. Furthermore, Sikadur 330 consistently generated a smoother failure surface, whereas Sikadur 30 LP exhibited a comparatively rougher texture. Fractographic assessment of specimens fabricated with Sikadur 30 LP and Sikadur 330 further reveals that, in Sikadur 330 specimens, failure cracks on either side of the specimen surface, typically run parallel to each other along the lateral wires. Near the failure plane, these cracks are closely spaced, with the distance between them increasing as one moves away from the failure zone. Conversely, in specimens prepared with Sikadur 30 LP, failure cracks exhibit a zigzag pattern along both sides of the surface. This irregular crack path suggests that Sikadur 30 LP allows for greater deformation before failure, potentially offering more favorable mechanical performance compared to Sikadur 330.

Bonding Material	Specimen Configuration	Average Ultimate Load kN	Average Ultimate Load (Half) for one side wraps kN	Average Displacement at Ultimate Load mm	Average Stiffness kN/mm	Average Bond Strength N/mm²	Average Rupture Strain μm/m
Sikadur 30 LP	GG	43.42	21.71	3.65	12.61	90.84	3379
	GS	56.82	28.41	7.53	8.61	127.97	9725
	SG	46.36	23.18	6.45	9.34	104.41	9107
	SS	19.90	9.95	5.57	3.91	50.00	8259
	GGG	67.64	33.82	3.98	17.23	115.82	3954
	GSG	57.98	28.99	5.23	12.25	103.54	5940
	SGS	52.22	26.11	6.03	10.68	107.89	8488
	SSS	27.86	13.93	6.25	4.78	51.40	8990
Sikadur 330	GG	32.68	16.34	3.57	10.43	77.08	3309
	GS	28.78	14.39	5.15	6.39	69.18	7751
	SG	26.38	13.19	5.03	5.73	63.41	7583
	SS	17.08	8.54	5.38	3.38	44.02	8007
	GGG	42.98	21.49	3.71	13.03	77.86	3720
	GSG	40.22	20.11	4.59	9.45	77.95	5848
	SGS	34.08	17.04	5.01	7.96	73.45	7495
	SSS	23.08	11.54	5.54	4.51	46.16	8190

Table 6: Results of the bond test performed on dumbbell specimens.

Bond test on dumbbell specimens

The bond test results, including ultimate load, displacement at ultimate load, rupture strain and stiffness are presented in Tab. 6. A total of 48 dumbbell specimens are cast, strengthened and tested to evaluate the bond strength between concrete and the strengthening layer under ambient room temperature conditions. These specimens are divided into two primary groups according to the type of adhesive i.e. Sikadur 30 LP and Sikadur 330. Additionally, each group is further subdivided based on various strengthening configurations, including GG, GS, SG, SS, GGG, GSG, SGS, and SSS, to assess their influence on the bond performance of specimen. Three specimens are considered for each configuration and average results of three specimens are presented in Tab. 6. In addition to average values, standard deviation and coefficient of variance for different strengthening configuration used for bond test are shown in Tab. 7. The majority of the specimens exhibit CoV

values below 5%, indicating high consistency and reliability of the bond test results. Although slightly higher CoV values are observed for the ultimate load and bond strength in the SGS configuration and for rupture strain in SS configuration, however they also remain within acceptable experimental limit. These findings, combined with narrow confidence intervals observed in graphical data representations, affirm the consistency and repeatability of the results.

Epoxy	Specimen Configuration	Ultimate Load		Bond Strength		Stiffness		Rupture Strain	
		SD	CoV (%)	SD	CoV (%)	SD	CoV (%)	SD	CoV (%)
Sikadur 30LP	GG	1.65	3.80	3.45	3.80	106.36	4.58	0.58	3.15
	GS	0.57	1.00	1.28	1.00	152.44	1.88	0.16	1.57
	SG	1.99	4.30	4.49	4.30	137.76	1.23	0.11	1.51
	SS	0.90	4.51	2.25	4.51	304.12	0.82	0.03	3.68
	GGG	1.83	2.70	3.13	2.70	219.89	2.72	0.47	5.56
	GSG	0.88	1.51	1.57	1.51	205.91	1.63	0.20	3.47
	SGS	4.14	7.93	8.56	7.93	382.46	3.04	0.33	4.51
	SSS	0.65	2.33	1.20	2.33	195.72	1.53	0.07	2.18
Sikadur 330	GG	1.10	3.36	2.59	3.36	228.19	1.75	0.18	6.90
	GS	0.96	3.33	2.30	3.33	147.54	2.29	0.15	1.90
	SG	0.86	3.25	2.06	3.25	294.14	2.82	0.16	3.88
	SS	0.56	3.28	1.44	3.28	821.48	2.58	0.09	10.26
	GGG	0.94	2.19	1.70	2.19	179.62	2.85	0.37	4.83
	GSG	1.58	3.92	3.05	3.92	193.18	5.81	0.55	3.30
	SGS	1.70	4.98	3.66	4.98	482.20	2.74	0.22	6.43
	SSS	0.19	0.84	0.39	0.84	303.63	3.66	0.17	3.71

SD = standard deviation, CoV - coefficient of variance

Table 7: Statistical indicators for mechanical parameters obtained from bond tests.

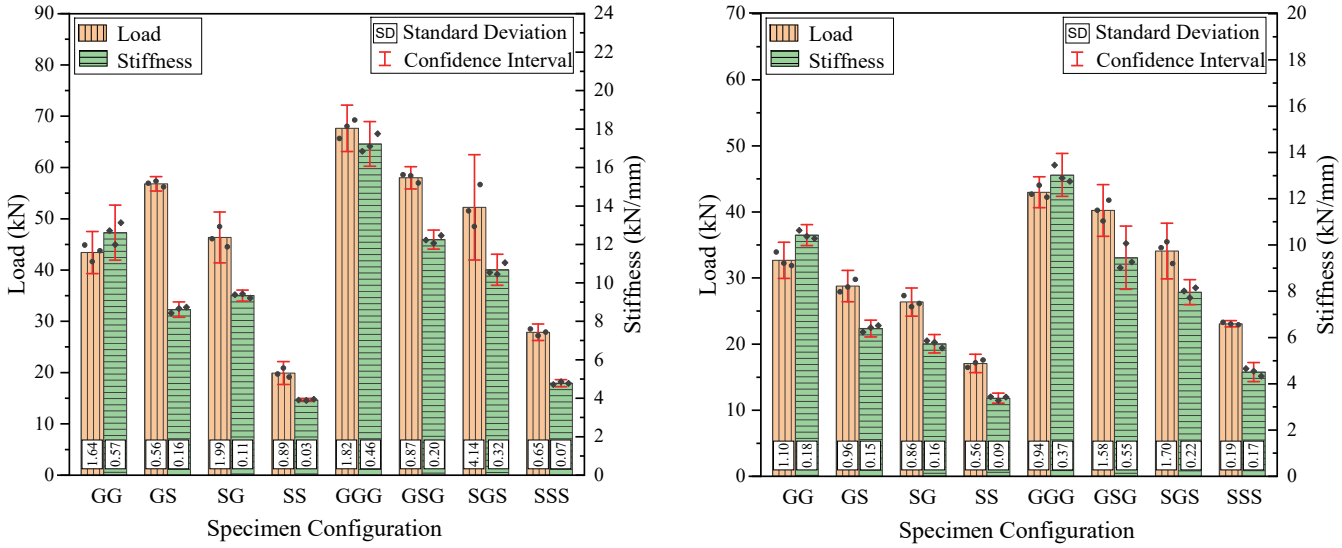

(a) use of Sikadur 30 LP adhesive

(b) use of Sikadur 330 adhesive

Figure 15: Comparison of ultimate load and stiffness for dumbbell specimens with different strengthening configuration

Comparison of ultimate load capacity and stiffness for dumbbell specimen strengthened using different configurations using Sikadur 30 LP and Sikadur 330 is presented in bar chart form in Fig. 15. A comparative evaluation of the two-layer and three-layer specimens reveals the superior performance of hybrid wrap configurations. Among the two-layer wraps, the GS and SG configurations, demonstrated higher load carrying capacity as compared to the GG and SS specimen. For specimens prepared using Sikadur 30 LP, GS recorded an average ultimate load of 56.82 kN, which is 30.86% higher than 43.42 kN of GG and nearly 2.85 times higher than 19.90 kN of SS. Similarly, ultimate load capacity of SG is 46.36 kN, surpassing GG by 6.77% and 2.33 times higher as compared to SS. This indicates that the hybrid wraps are effectively enhances bond behaviour. The hybrid benefit is still evident, when adhesive Sikadur 330 is used. Specimen GS and SG recorded 28.78 kN and 26.38 kN, respectively, while GG and SS showed 32.68 kN and 17.08 kN. Although GS and SG are slightly lower than

GG in this case, they perform better than SS by 68.50% and 54.45%, respectively, emphasizing the advantage of hybridization over use of individual material. In the case of three-layer wraps, a similar trend is observed. The hybrid configurations GSG and SGS performed better than SSS and approached around 77% - 93% strength of the GGG. For Sikadur 30 LP, GSG and SGS achieved ultimate loads of 57.98 kN and 52.22 kN, respectively, which are 108.11% and 87.44% higher than 27.86 kN of SSS. Although, the load capacity of both is lower than 67.64 kN of GGG, they still offer a balance of strength and potential ductility due to the presence of SSWM. For Sikadur 330, GSG and SGS recorded 40.22 kN and 34.08 kN, representing 74.26% and 47.66% enhancement in ultimate load capacity over 23.08 kN of SSS. The data clearly supports the use of GFRP-SSWM hybrid configurations in structural strengthening applications, particularly when using Sikadur 30 LP, which yields better bonding as compared to Sikadur 330.

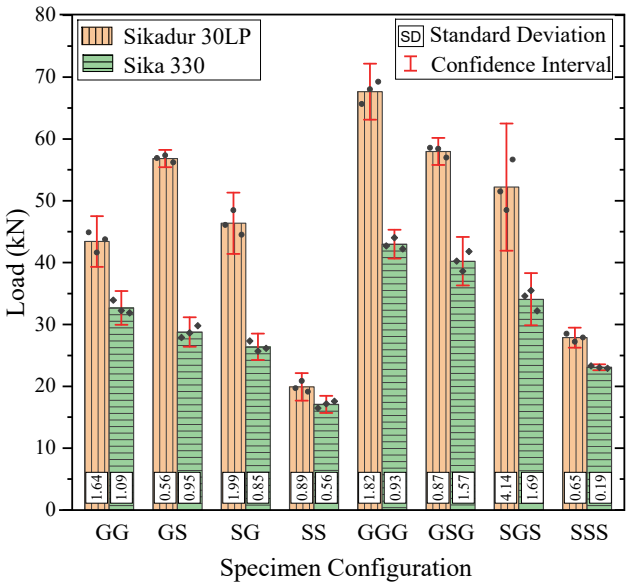

(a) Ultimate load capacity

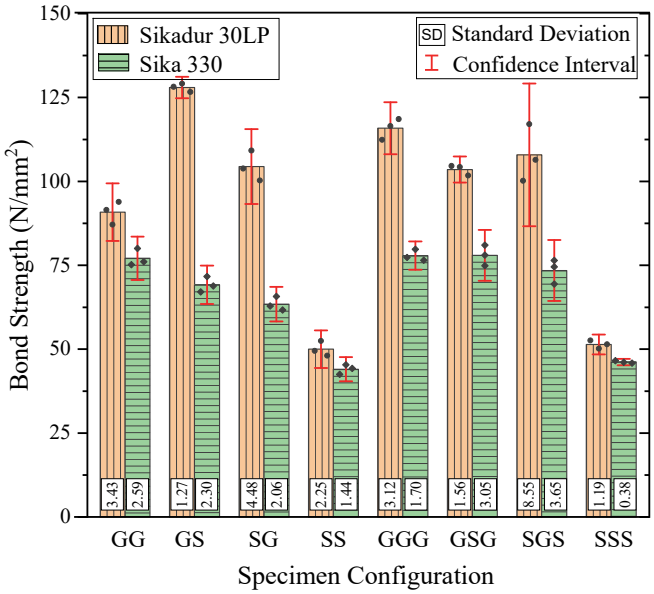

(b) Bond strength

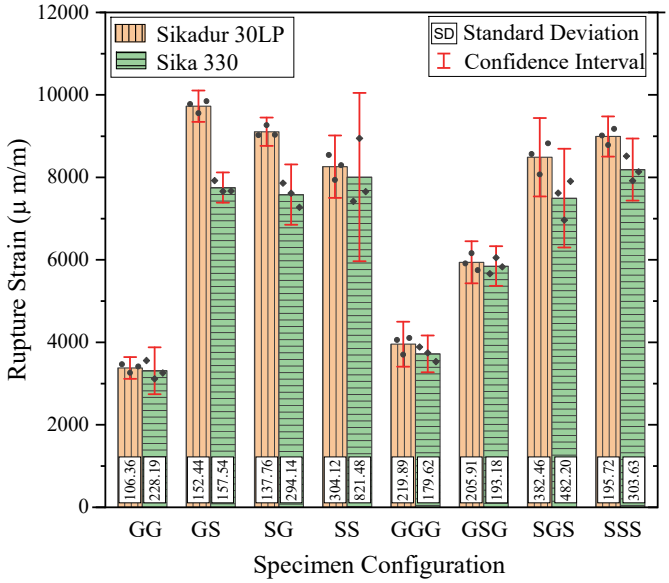

(c) Rupture strain

Figure 16: Comparison of results for dumbbell specimens with different strengthening configuration.

A comparison of ultimate load capacity, bond strength and rupture strain for all the specimen configurations prepared using Sikadur 30 LP and Sikadur 330 is presented in in Fig. 16(a) to Fig. 16(c). Overall, specimens prepared with Sikadur 30 LP is having higher ultimate load capacity than those prepared with Sikadur 330, highlighting superior adhesive performance of

Sikadur 30 LP. Among all configurations, the GGG specimen prepared with Sikadur 30 LP exhibited the highest average ultimate load of 67.64 kN, which is approximately 57.37% higher than its Sikadur 330 counterpart (42.98 kN). For GG specimen, 32.86% increase in ultimate load capacity is observed, when prepared using Sikadur 30 LP (43.42 kN) as compared to Sikadur 330 (32.68 kN). Similarly, the GS configuration with Sikadur 30 LP achieved an average ultimate load of 56.82 kN, which is 97.43% higher than the 28.78 kN ultimate load observed for Sikadur 330. The SG, SGS and GSG specimens also showed significant improvements with Sikadur 30 LP, registering 75.74%, 53.22% and 44.16% higher ultimate loads, respectively, compared to Sikadur 330. The differences are less pronounced in the SS and SSS configurations, where both adhesives showed relatively low bond strengths. However, Sikadur 30 LP still outperformed Sikadur 330, with improvements of 16.5% and 20.7%, respectively. These findings suggest that Sikadur 30 LP offers a more robust bond, especially in hybrid or fiber-dominated configurations where better mechanical interlocking and adhesive penetration are critical. Notably, the GG specimen showed an increase of 32.9% in ultimate load when using Sikadur 30 LP compared to Sikadur 330. The data clearly support that Sikadur 30 LP is more effective across most configurations, particularly in those involving metallic or mixed reinforcement layers. This can be attributed to its lower viscosity, which likely enables better penetration and bonding with the stainless-steel wire mesh (SSWM), resulting in higher bond strength and improved load transfer efficiency.

The bond strength is calculated as the ratio of the ultimate load to the laminate area, which slightly varies across different configurations and adhesives. For specimens bonded using Sikadur 30 LP, higher bond strength values are consistently observed, as shown in Fig. 16(b), compared to those bonded with Sikadur 330, indicating superior bonding performance of Sikadur 30 LP. Among all configurations, the GS specimen bonded with Sikadur 30 LP exhibits the highest bond strength of 127.97 N/mm², demonstrating effective load transfer and strong adhesion in hybrid arrangements. Similar trend is also observed for rupture strain. Higher values of rupture strain are observed for specimens prepared using Sikadur 30 LP as compared to their Sikadur 330 counterparts. Due to brittle behaviour of GFRP, the specimens strengthened with GFRP-only wraps i.e. GG and GGG exhibit lowers rupture strain, despite having higher load carrying capacity. On the contrary, higher values of rupture strain for SS and SSS specimens, demonstrate their ductile behaviour, though load carrying capacity is relatively lesser.

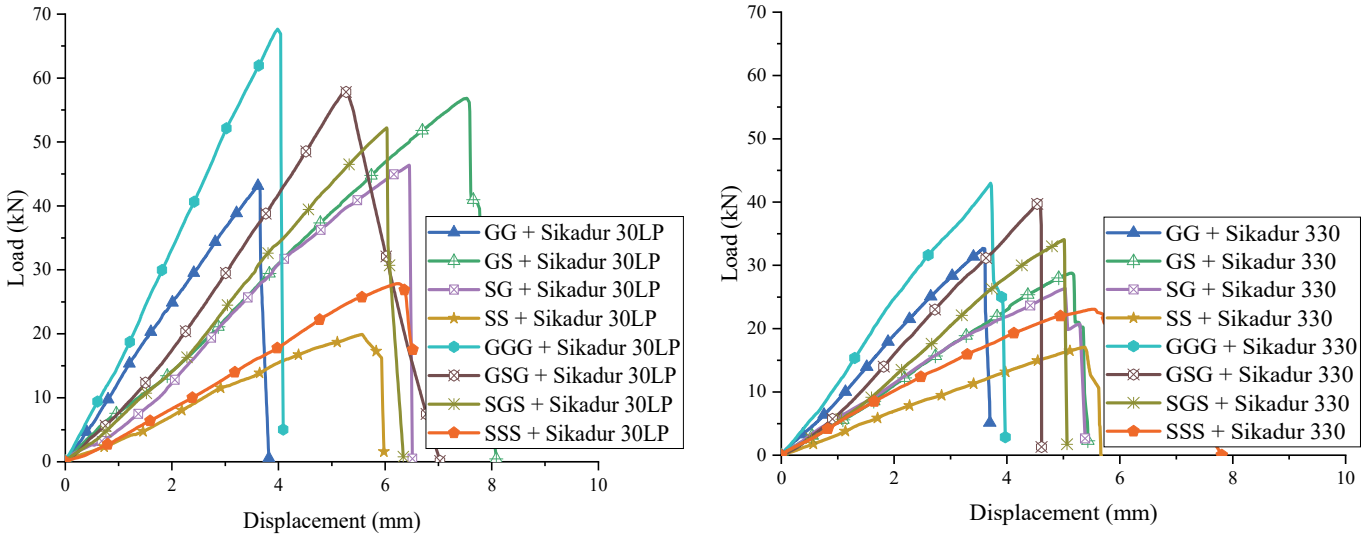

(a) strengthening using Sikadur 30 LP adhesive

(b) strengthening using Sikadur 330 adhesive

Figure 17: Load vs. displacement response of dumbbell specimens with different strengthening configuration.

A graph of ultimate load vs. deflection is presented in Fig. 17. From the graph, it is observed that specimens GG and GGG is lacking ductility, despite high load carrying capacity. They typically demonstrate stiffer but more brittle response with limited post peak ductility. On the contrary, for SS and SSS specimens, ductility is more though load carrying capacity is lesser. Hybrid specimen GS, when prepared using Sikadur 30 LP is having a slightly lower ultimate load capacity of 56.82 kN than GG, but it shows the highest displacement of 7.53 mm at failure, suggesting a ductile failure mode and better energy absorption. The hybrid specimens i.e. GS, SG, SGS, and GSG demonstrate a more balanced performance between strength and ductility. For instance, SG exhibited a peak load of 46.36 kN with a deflection of 6.45 mm, and GSG recorded 57.98 kN and 5.23 mm, respectively. Similar trend is also observed for specimens prepared using Sikadur 330. Among two-layer specimen, GS (5.15 mm) and SG (5.03 mm) shows higher displacement by 44.26% and 40.89%, respectively, as compared

to GG (3.57 mm). Three-layer hybrid specimens GSG (4.59 mm) and SGS (5.01 mm) also surpassed GGG (3.71 mm) in ductility, confirming the beneficial role of hybrid wraps. These results, both visually in the Fig. 17 and Tab. 6, highlight that provision of SSWM in combination with GFRP improves ductility without significantly compromising on strength.

Strain values are also measured during experimental studies with the help of 5 mm gauge length electrical resistance strain gauge. A graph of load vs. strain is shown in Fig. 18 and values of rupture strain for different specimen configurations are summarized in Tab. 6. Hybrid wraps demonstrates improved rupture strain values compared to their non-hybrid counterparts. Among the two-layer configurations, the GS specimen, when prepared using Sikadur 30 LP exhibits the highest rupture strain of 9725 μm/m, indicating its ductile performance. This value is 6.78% higher than SG (9107 μm/m), 17.75% greater than the SS (8259 μm/m) and 187.81% higher than GG specimen. In three-layer configurations, SGS and GSG specimens showed rupture strains of 8488 μm/m and 5940 μm/m, respectively. Compared to the SSS (8990 μm/m) and GGG (3954 μm/m), the SGS specimen stands out with a more balanced performance, achieving more than double the rupture strain of GGG. Overall, with similar trend, lower rupture strain values are observed for specimens prepared with Sikadur 330 as compared to Sikadur 30 LP. Highest rupture strain values are observed for specimen SS and SSS, when prepared using Sikadur 330. Among, hybrid configurations, specimen GS and specimen SGS performs superior as compared to specimen SG and GSG.

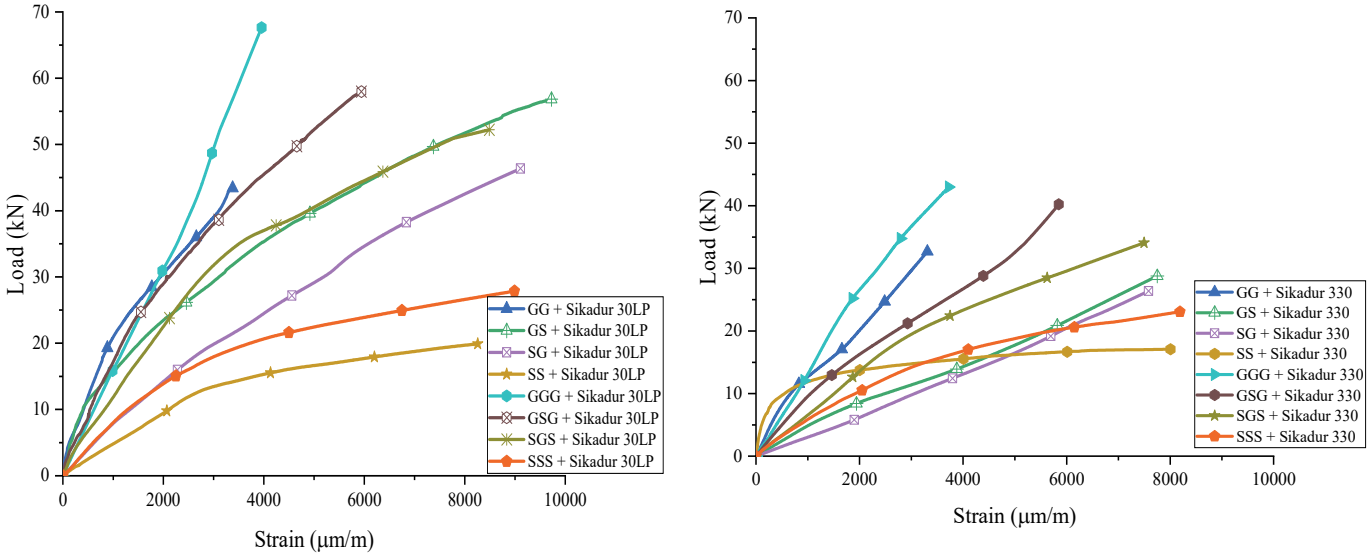

(a) strengthening using Sikadur 30 LP adhesive

(b) strengthening using Sikadur 330 adhesive

Figure 18: A graph of load vs. strain for dumbbell specimens with different strengthening configuration

Failure pattern of dumbbell specimens

Fig. 19 illustrates the observed typical failure patterns observed for dumbbell specimen strengthened with different configurations of GFRP and SSWM using Sikadur 30 LP (Fig. 19a) and Sikadur 330 (Fig. 19b). From the varied failure photographs, it is observed that, type of epoxy adhesive and strengthening layers configuration, significantly influence the bond performance of the specimen. Tearing of SSWM is observed for specimen SS strengthened using both Sikadur 30 LP and Sikadur 330 without any significant debonding, which indicates that full strength of SSWM is utilized in load resistance maintaining proper bond. On the contrary, for specimen GG and GGG, debonding of wraps is observed without any major failure in it, along with failure of concrete portion of dumbbell specimen, due to high load carrying capacity and strength of GFRP layers. Debonding at the interface between the adhesive layer and concrete is observed for almost all the specimens, when prepared using Sikadur 330, which suggest superior bond behaviour of specimen using Sikadur 30 LP. From the failure photographs, it is further observed that, two-layer wraps demonstrate more effective bond characteristics as compared to three-layer wraps.

Fig. 20 represents a schematic diagram showing the possible failure locations in the strengthened dumbbell specimen. In the SS, GS, and SSS specimens prepared using Sikadur 30 LP, failure occurs at the center, near the 1 mm slit between the two concrete parts of dumbbell specimen, without any noticeable delamination between the layers. This suggests effective hybrid action, especially in the GS specimen. For the SG specimen strengthened with Sikadur 30 LP, failure is observed near the center with a clear separation between the SSWM and GFRP layers at the later stage of loading. Additionally, rupture of the GFRP layer is visible, indicating good stress transfer between the two materials through the adhesive layer.

In the GG specimen prepared using Sikadur 30 LP, failure occurs at the concrete - adhesive interface. For the GSG, SGS, and GGG specimens bonded with Sikadur 30 LP, the failure primarily involves the concrete substrate near the specimen edges with debonding of strengthening layer. For the SS specimen bonded with Sikadur 330 exhibits tearing of the SSWM layer at the central slit without any evident debonding. For all other Sikadur 330 specimens, clear debonding between the concrete and laminate is observed, along with concrete failure at the specimen edges. These failure modes suggest that the concrete fails before the full-strength utilization of the strengthening materials, particularly when using Sikadur 330.

SS SG GS GG SSS SGS GSG GGG

(a) strengthening using Sikadur 30 LP

SS SG GS GG SSS SGS GSG GGG

(b) strengthening using Sikadur 330

Figure 19: Typical failure patterns of dumbbell specimens during bond test.

The capacity utilization ratio, calculated as the ratio of the average ultimate load on one side of the dumbbell bond specimens to the average ultimate load from tensile coupon tests is presented in Tab. 8, for various strengthening configurations using Sikadur 30 LP and Sikadur 330. The results reveal that specimens strengthened exclusively with GFRP (GG and GGG) utilize only around 40% of their material tensile capacity in load resistance. In these cases, failure occurs due to concrete crushing and subsequent debonding of laminate layer with concrete surface, before the full strength of the strengthening material is utilized. In contrast, specimens strengthened with SSWM (SS and SSS) demonstrate significantly higher capacity utilization, exceeding 83% with Sikadur 330 and approaching 90% with Sikadur 30 LP. This indicates a strong bond between the SSWM and the concrete surface. It further suggests that nearly the full tensile capacity of SSWM is effectively engaged, especially when bonded using Sikadur 30 LP. While hybrid specimens show moderate capacity utilization (around 45% to

50%) when bonded with Sikadur 330, much higher performance is observed with Sikadur 30 LP. Specifically, GS specimens achieve nearly 90% capacity utilization and SG specimens about 73%, highlighting the superior bonding efficiency and load transfer capability of Sikadur 30 LP in GFRP-SSWM hybrid wraps. These observations highlight the enhanced performance of Sikadur 30 LP compared to Sikadur 330 across various configurations.

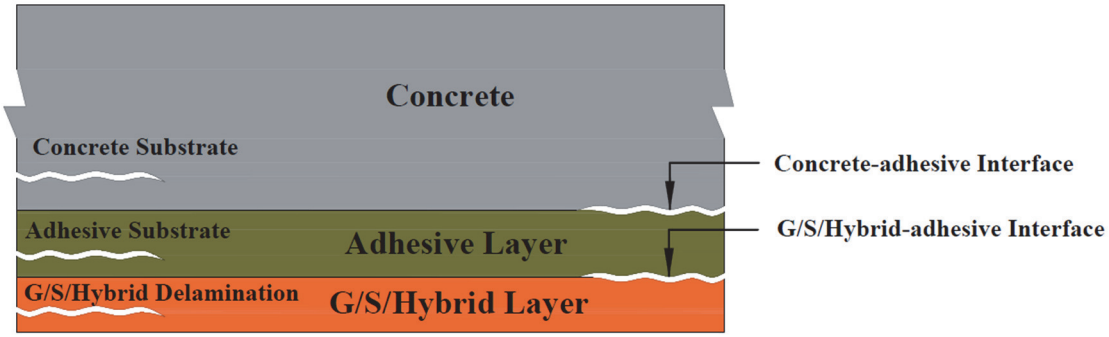

Figure 20: Schematic representation of possible failure location of strengthened specimen.

Specimen Configuration	Sikadur 30 LP			Sikadur 330		
	Average Ultimate Load observed during tensile test (UL_T)	Average Ultimate Load for one side wrap observed during bond test (UL_B)	Capacity Utilization Ratio (UL_B/ UL_T)	Average Ultimate Load observed during tensile test (UL_T)	Average Ultimate Load for one side wrap observed during bond test (UL_B)	Capacity Utilization Ratio (UL_B/ UL_T)
	kN	kN	%	kN	kN	%
GG	50.25	21.71	43.20	44.99	16.34	36.32
GS	31.74	28.41	89.51	29.20	14.39	49.28
SG	31.74	23.18	73.03	29.20	13.19	45.17
SS	10.45	9.95	95.22	9.90	8.54	86.26
GGG	62.23	33.82	54.35	61.43	21.49	34.98
GSG	55.67	28.99	52.07	48.28	20.11	41.65
SGS	36.20	26.11	72.13	34.27	17.04	49.72
SSS	15.56	13.93	89.52	13.75	11.54	83.93

Table 8: Results of capacity utilization ratio.

CONCLUSIONS

This study presented an experimental investigation on 42 coupon specimens and 48 dumbbell specimens to assess the mechanical performance of various hybrid GFRP-SSWM wrap configurations, prepared using two epoxy adhesives i.e. Sikadur 30 LP and Sikadur 330. Based on the experimental outcomes, the following conclusions are drawn:

- The failure modes observed in hybrid coupon specimens confirm that effective hybrid behavior is achieved using the hand layup technique adopted in this study for development of hybrid coupon specimen.
- Results from tensile and bond tests, along with fractographic analysis, indicate that Sikadur 30 LP is more suitable and effective for hybrid specimens, particularly those incorporating SSWM. Sikadur 330 shows better compatibility with GFRP-only configurations.
- Failure patterns of dumbbell specimen and capacity utilization analysis reveals that the full tensile strength of GFRP layers is not utilized in GFRP-only configurations, due to debonding and failure of the concrete portion beneath the bonded layer.

- GFRP-only specimens exhibit higher load-carrying capacity and stiffness but fail in a brittle manner with lower rupture strain and ductility. In contrast, SSWM-only specimens display greater ductility and rupture strain but lower strength and stiffness.
- Hybrid wraps offer a balanced response in terms of strength and ductility. Among two-layer hybrid configurations, the GS configuration performs better than SG.
- Two-layer hybrid configurations are generally recommended over three-layer wraps, as increasing the number of layers can introduce brittleness and reduce overall ductility.

The present study primarily focuses on evaluating the tensile and bond behavior of GFRP-SSWM hybrid wraps using small-scale laboratory specimens under static loading conditions. However, further studies can be conducted to evaluate the performance of GFRP-SSWM hybrid wraps in structural strengthening applications such as flexural or shear enhancement of RC beams and confinement of columns, incorporating a wider range of epoxy adhesives. Additionally, the effects of environmental factors such as moisture, corrosion, and temperature variation on the performance of hybrid wraps requires further investigation. Long-term durability studies of RC elements strengthened with hybrid wraps, including corrosion resistance and behavior under elevated temperatures or fire exposure, are also recommended. Moreover, evaluating the performance of hybrid wraps under cyclic, fatigue, or dynamic loading, as well as in full-scale structural elements, can be scope for future research.

ACKNOWLEDGEMENT

The authors gratefully acknowledge the financial support provided by Nirma University under the scheme of Minor Research Project (sanction no. NU/DRI/MinResPrj/IT/2022-23 dated 10/02/2022) for conducting an experimental work presented in this paper.

REFERENCES

[1] Ahmed, A., Zillur Rahman, M., Ou, Y., Liu, S., Mobasher, B., Guo, S., Zhu, D. (2021). A review on the tensile behavior of fiber-reinforced polymer composites under varying strain rates and temperatures, Constr. Build. Mater., 294, DOI: https://doi.org/10.1016/j.conbuildmat.2021.123565.

[2] Siddika, A., Mamun, M.A. Al., Ferdous, W., Alyousef, R. (2020). Performances, challenges and opportunities in strengthening reinforced concrete structures by using FRPs – A state-of-the-art review, Eng. Fail. Anal., 111, DOI: https://doi.org/10.1016/j.engfailanal.2020.104480.

[3] Swolfs, Y., Gorbatikh, L., Verpoest, I. (2014). Fibre hybridisation in polymer composites: A review, Compos. Part A, 67, pp. 181–200, DOI: https://doi.org/10.1016/j.compositesa.2014.08.027.

[4] Hawileh, R.A., Abu-Obeidah, A., Abdalla, J.A., Al-Tamimi, A. (2015). Temperature effect on the mechanical properties of carbon, glass and carbon-glass FRP laminates, Constr. Build. Mater., 75, pp. 342–348, DOI: https://doi.org/10.1016/j.conbuildmat.2014.11.020.

[5] Wu, Z., Wang, X., Iwashita, K., Sasaki, T., Hamaguchi, Y. (2010). Tensile fatigue behaviour of FRP and hybrid FRP sheets, Compos. Part B Eng., 41(5), pp. 396–402, DOI: https://doi.org/10.1016/j.compositesb.2010.02.001.

[6] Chaturvedi, K.C., Chittappa, H.C. (2021). Study of tensile nature of jute hybrid composite by the variation of S-glass fibers- an outlook from experimental perspective, Mater. Today Proc., 46, pp. 2783–2786, DOI: https://doi.org/10.1016/j.matpr.2021.02.593.

[7] McBride, A.K., Turek, S.L., Zaghi, A.E., Burke, K.A. (2017). Mechanical Behavior of Hybrid Glass/Steel Fiber Reinforced Epoxy Composites, Polymers (Basel)., 9(4), DOI: https://doi.org/10.3390/polym9040151.

[8] Phaneendra, A.N., Sankaraiah, G., Reddy, V.D., Reddy, R.M. (2021). Assimilation of Mechanical properties of reinforced aluminum, stainless steel wire mesh with glass fiber epoxy hybrid composites for aircraft application, Adv. Mater. Process. Technol., 7(2), pp. 288–303, DOI: https://doi.org/10.1080/2374068X.2020.1765107.

[9] Khalid, M.Y., Al Rashid, A., Arif, Z.U., Sheikh, M.F., Arshad, H., Nasir, M.A. (2021). Tensile strength evaluation of glass/jute fibers reinforced composites: An experimental and numerical approach, Results Eng., 10, DOI: https://doi.org/10.1016/j.rineng.2021.100232.

[10] Saidane, E.H., Scida, D., Assarar, M., Sabhi, H., Ayad, R. (2016). Hybridisation effect on diffusion kinetic and tensile mechanical behaviour of epoxy based flax–glass composites, Compos. Part A, 87, pp. 153–160, DOI: https://doi.org/10.1016/j.compositesa.2016.04.023

[11] ACI, C. 440. (2017). ACI 440.2R-17: Guide for the Design and Construction of Externally Bonded FRP Systems for Strengthening Concrete Structures, .
[12] Obaidat, Y.T., Heyden, S., Dahlblom, O. (2013). Evaluation of Parameters of Bond Action between FRP and Concrete, J. Compos. Constr., 17(5), pp. 626–635, DOI: https://doi.org/10.1061/(asce)cc.1943-5614.0000378.
[13] McIsaac, A., Mak, K., Fam, A. (2019). Influence of Resin Biocontent and Type on Bond Strength between FRP Wet Layup and Concrete, J. Compos. Constr., 23(4), DOI: https://doi.org/10.1061/(asce)cc.1943-5614.0000955.
[14] Nakaba, K., Kanakubo, T., Furuta, T., Yoshizawa, H. (2001). Bond behavior between fiber-reinforced polymer laminates and concrete, ACI Struct. J., 98(3), pp. 359–367, DOI: https://doi.org/10.14359/10224.
[15] Yuan, C., Chen, W., Pham, T.M., Hao, H. (2019). Bond behaviour between hybrid fiber reinforced polymer sheets and concrete, Constr. Build. Mater., 210, pp. 93–110, DOI: https://doi.org/10.1016/j.conbuildmat.2019.03.082.
[16] Huang, S., Yan, L., Bachtiar, E.V., Gao, C., Kasal, B. (2022). Bond behaviour between flax-glass hybrid fibre reinforced epoxy composite and laminated veneer lumber joints, J. Build. Eng., 50, pp. 104207, DOI: https://doi.org/10.1016/j.jobe.2022.104207.
[17] Choobbora, S.S., Hawileh, R.A., Abu-Obeidah, A., Abdalla, J.A. (2019). Performance of hybrid carbon and basalt FRP sheets in strengthening concrete beams in flexure, Compos. Struct., 227, pp. 111337-1-11, DOI: https://doi.org/10.1016/j.compstruct.2019.111337.
[18] Bai, Y.L., Niu, W.Q., Mei, S.J., Gao, W.Y. (2025). Flexural behavior of hybrid C-PET FRP-strengthened RC beams with U-strip anchorages, Eng. Struct., 322, pp. 119164-1-17, DOI: https://doi.org/10.1016/j.engstruct.2024.119164.
[19] Lin, B., Chun, Q., Mi, Z. (2024). Flexural behavior of historical RC beams strengthened with hybrid FRP sheets, Case Stud. Constr. Mater., 20, pp. e03410-1-20, DOI: https://doi.org/10.1016/j.cscm.2024.e03410.
[20] Xiong, G.J., Yang, J.Z., Ji, Z.B. (2004). Behavior of reinforced concrete beams strengthened with externally bonded hybrid carbon fiber–glass fiber sheets, J. Compos. Constr., 8(3), pp. 275–278, DOI: https://doi.org/10.1061/(ASCE)1090-0268(2004)8:3(275).
[21] Kumar, V., Patel, P. V. (2016). Strengthening of axially loaded circular concrete columns using stainless steel wire mesh (SSWM) – Experimental investigations, Constr. Build. Mater., 124, pp. 186–198, DOI: https://doi.org/10.1016/j.conbuildmat.2016.06.109.
[22] Raiyani, S.D., Patel, P., Prakash, S.S. (2024). Effectiveness of partial wrapping of stainless-steel wire mesh on compression behavior of concrete cylinders, Frattura ed Integrità Strutturale, 18(69), pp. 71–88, DOI: https://doi.org/10.3221/IGF-ESIS.69.06.
[23] Ferro, P., Fabrizi, A., Bonollo, F., Berto, F. (2020). Microstructural and mechanical characterization of a stainless-steel wire mesh–reinforced Al-matrix composite, Frattura ed Integrità Strutturale, 15(55), pp. 289–301, DOI: https://doi.org/10.3221/IGF-ESIS.55.22.
[24] Harba, I., Abdulridha, A., AL-Shaar, A. (2022). Numerical analysis of reinforced concrete circular columns strengthening with CFRP under concentric and eccentric loadings, Frattura ed Integrità Strutturale, 17(63), pp. 190–205, DOI: https://doi.org/10.3221/IGF-ESIS.63.16.
[25] ASTM D3039/D3039-M. (2014). Astm D3039/D3039M Standard Test Method for Tensile Properties of Polymer Matrix Composite Materials, Annu. B. ASTM Stand., pp. 1–13, DOI: https://doi.org/10.1520/D3039.